COMPRESSIVE INVERSE SCATTERING I. HIGH FREQUENCY SIMO/MIMO MEASUREMENTS

ALBERT C. FANNJIANG

Abstract. Inverse scattering from discrete targets with the single-input-multiple-output (SIMO), multiple-input-single-output (MISO) or multiple-input-multiple-output (MIMO) measurements is analyzed by compressed sensing theory with and without the Born approximation.

High frequency analysis of (probabilistic) recoverability by the L^1-based minimization/regularization principles is presented. In the absence of noise, it is shown that the L^1-based solution can recover exactly the target of sparsity up to the dimension of the data either with the MIMO measurement for the Born scattering or with the SIMO/MISO measurement for the exact scattering. The stability with respect to noisy data is proved for weak or widely separated scatterers. Reciprocity between the SIMO and MISO measurements is analyzed. Finally a coherence bound (and the resulting recoverability) is proved for diffraction tomography with high-frequency, few-view and limited-angle SIMO/MISO measurements.

1. Introduction

A monochromatic wave u propagating in a heterogeneous medium characterized by a variable refractive index $n = \sqrt{1+\nu}$ is governed by the Helmholtz equation

$$\Delta u(\mathbf{r}) + \omega^2(1+\nu(\mathbf{r}))u(\mathbf{r}) = 0 \tag{1}$$

where $\nu \in \mathbb{C}$ describes the medium inhomogeneities. For simplicity, the wave velocity is assumed to be unity and hence the wavenumber ω equals the frequency.

Consider the plane wave incidence

$$u^{\rm i}(\mathbf{r}) = e^{i\omega \mathbf{r}\cdot\mathbf{d}} \tag{2}$$

where $\mathbf{d} \in S^{d-1}, d = 2, 3$, is the incident direction. The scattered field $u^{\rm s} = u - u^{\rm i}$ then satisfies

$$\Delta u^{\rm s} + \omega^2 u^{\rm s} = -\omega^2 \nu u \tag{3}$$

which can be written as the Lippmann-Schwinger equation:

$$u^{\rm s}(\mathbf{r}) \;=\; \omega^2 \int_{\mathbb{R}^d} \nu(\mathbf{r}') \left(u^{\rm i}(\mathbf{r}') + u^{\rm s}(\mathbf{r}')\right) G(\mathbf{r},\mathbf{r}')d\mathbf{r}' \tag{4}$$

where G is the Green function for the operator $-(\Delta+\omega^2)$ (see Appendix A for the reciprocal formulation).

The scattered field has the far-field asymptotic [35]

$$u^{\rm s}(\mathbf{r}) = \frac{e^{i\omega|\mathbf{r}|}}{|\mathbf{r}|^{(d-1)/2}} \left(A(\hat{\mathbf{r}},\mathbf{d}) + \mathcal{O}\left(\frac{1}{|\mathbf{r}|}\right)\right), \quad \hat{\mathbf{r}} = \mathbf{r}/|\mathbf{r}|, \quad d = 2,3 \tag{5}$$

where the scattering amplitude A is determined by the formula [44]

$$A(\hat{\mathbf{r}},\mathbf{d}) \;=\; \frac{\omega^2}{4\pi} \int_{\mathbb{R}^d} \nu(\mathbf{r}')u(\mathbf{r}')e^{-i\omega\mathbf{r}'\cdot\hat{\mathbf{r}}}d\mathbf{r}'. \tag{6}$$

In the inverse scattering theory, the scattering amplitude is the observable data and the main objective then is to reconstruct ν from the knowledge of the scattering amplitude. In this paper,

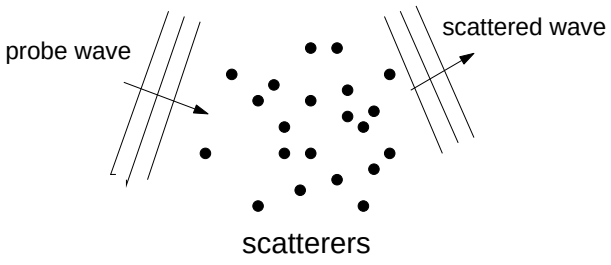

FIGURE 1. Far-field imaging geometry

we use the L^1-minimization principle called the *Basis Pursuit* to study the inverse scattering from point scatterers. Note that since u in (6) is part of the unknown, the inverse scattering problem is nonlinear. Physically speaking, the nonlinearity is the consequence of multiple scattering among the different scatterers.

The standard theory of inverse scattering asserts the injectivity of the mapping from $\nu \in C_c^1$ with a nonnegative imaginary part to the corresponding scattering amplitude for a fixed frequency in *three* (or higher) dimensions (Theorem 5.5 of [13]. See also [24, 35, 40, 41, 43] for similar results, [29, 37, 38, 45] for inverse boundary-value problem and [14, 30, 31, 35] for inverse obstacle scattering). In this case, the refractive index can be determined uniquely by the full knowledge of $A(\hat{\mathbf{r}}, \mathbf{d}), \forall \mathbf{d}, \hat{\mathbf{r}}$, for a fixed ω. Indeed, as A is analytic in both $\mathbf{d}$ and $\hat{\mathbf{r}}$, it suffices to know A for a countably many incident and sampling directions in order to determine ν uniquely. As far as we know, the uniqueness in two dimensions with a fixed frequency is still an open question. What is known for two dimensions is that the uniqueness holds if the scattering amplitude is given for an interval of frequencies [13].

Of obvious theoretical interest, the uniqueness result by itself is of limited practical interest. All existing methods for determining the refractive index without linearizing the problem are based on the constrained nonlinear optimization in the L^2-norm for which the exact recoverability is usually difficult to establish, especially in the case of undersampling [13, 14]. In this paper we show that a target is the unique, global minimizer of an optimization principle based on the L^1-norm if the target satisfies certain sparsity constraint. Moreover, this L^1-minimization problem can be effectively solved by linear programming as well as various low-complexity greedy algorithms.

In this paper we focus on the two dimensional setting ($\mathbf{r} = (x, z) \in \mathbb{R}^2$) for the aforementioned reason as well as the notational simplicity. Although the details of the results are dimension-dependent, our approach is not limited to higher dimensions. We discuss the three dimensional case briefly in Sections 2.4 and 2.5.

Consider the medium with point scatterers located in a square lattice $\mathcal{L} = \{\mathbf{r}_i = (x_i, z_i) : i = 1, ..., m\}$ of spacing ℓ. The total number m of grid points in $\mathcal{L}$ is a perfect square. Without loss of generality, assume $x_j = j_1\ell, z_j = j_2\ell$ where $j = (j_1 - 1)\sqrt{m} + j_2$ and $j_1, j_2 = 1, ..., \sqrt{m}$. Let $\nu_j, j = 1, ..., m$ be the strength of the scatterers. Let $\mathcal{S} = \left\{\mathbf{r}_{i_j} = (x_{i_j}, z_{i_j}) : j = 1, ..., s\right\}$ be the locations of the scatterers. Hence $\nu_j = 0, \forall \mathbf{r}_j \notin \mathcal{S}$. When there is no risk of confusion, we shall write $\nu = (\nu_j)$ in the sequel.

The scattering amplitude for this medium is a finite sum

$$A(\hat{\mathbf{r}}, \mathbf{d}) = \frac{\omega^2}{4\pi} \sum_{j=1}^{m} \nu_j u(\mathbf{r}_j) e^{-i\omega \mathbf{r}_j \cdot \hat{\mathbf{r}}}. \tag{7}$$

Moreover, in analogy to (4), the exciting field $u(\mathbf{r}_{i_j})$ satisfies the Foldy-Lax equation [51, 36]

$$u(\mathbf{r}_{i_l}) \quad = \quad u^{\mathrm{i}}(\mathbf{r}_{i_l}) + \omega^2 \sum_{l \neq j} G(\mathbf{r}_{i_l}, \mathbf{r}_{i_j}) \nu_{i_j} u(\mathbf{r}_{i_j}), \quad l = 1, ..., s \tag{8}$$

where all the multiple scattering effects are included but the self field is excluded to avoid blow-up.

2. Methods and results

2.1. **MIMO Born scattering.** First consider the Born approximation to (7). In the Born approximation (also known as Rayleigh-Gans scattering in optics), the exciting field $u(\mathbf{r}_{i_j})$ is replaced by the incident field $u^{\mathrm{i}}(\mathbf{r}_{i_j})$. This approximation linearizes the relation between the the target strength and the scattering amplitude and is valid for sufficiently weak or widely separated scatterers.

For the Born scattering, we define the target vector $X = \nu \in \mathbb{C}^m$ and use multiple incident waves

$$u_k^{\mathrm{i}}(\mathbf{r}) = e^{i\omega(z \sin\theta_k + x \cos\theta_k)}, \quad k = 1, ..., p \tag{9}$$

where θ_k is the incident angle of the k-th probe wave. Throughout the paper we consider the single-input-multiple-output (SIMO), multiple-input-single-output (MISO) and the multiple-input-multiple-output (MIMO) measurements in which for each incident angle θ_k the resulting scattering amplitude is measured at the multiple sampling angles $\tilde{\theta}_l, l = 1, ..., n$. After normalization by $\omega^2/(4\pi)$, the totality of the collected data forms the measurement vector $Y \in \mathbb{C}^{pn}$. The corresponding sensing matrix in the linear relationship $Y = \mathbf{\Phi} X$ has the $(n(k-1)+l, j)$-entry

$$e^{-i\omega(z_j \sin\tilde{\theta}_l + x_j \cos\tilde{\theta}_l)} u_k^{\mathrm{i}}(\mathbf{r}_j). \tag{10}$$

where $\tilde{\theta}_l$ is the sampling angle of the l-th sensor.

Recent breakthrough in compressed sensing has established the insight that the target can be recovered exactly with nearly minimum sensing resources by the L^1-minimization principle, called basis pursuit (BP)

$$\min \|X\|_1 \qquad \text{s.t. } \mathbf{\Phi} X = Y \tag{11}$$

if the target is sufficiently sparse and the matrix $\mathbf{\Phi}$ satisfies either the incoherence property or the restricted isometry property [3, 5, 6, 8, 9, 11]. The L^1-minimization problem (11) can be solved by linear programming [2, 8, 11] or by various greedy algorithms [15, 39, 48].

In this paper we adopt the incoherence approach to analyzing the SIMO/MISO and MIMO inverse scattering problems. Previously we have shown in [21] that suitably designed SIMO and MIMO measurements with *planar* domains (in three dimensions) produce random partial Fourier matrix as the sensing matrix which possesses a nearly optimal restricted isometry constant (RIC) with respect to the sparsity of the target. Current compressed sensing theory predicts that (11) yields a superior performance [4, 9]. However, with non-planar domains the SIMO/MIMO measurements seem to produce a rather poor RIC. Hence we adopt the alternative approach of incoherence in this paper. The restricted isometry approach will be taken up in Part II for multi-shot SISO (single-input-single-output) measurements with non-planar domains for which the framework of random partial Fourier matrix can be restored by special sampling schemes.

To the best of our knowledge the present paper is the first rigorous study of inverse scattering, including multiple scattering, in the framework of compressed sensing. Earlier studies [10, 25, 32, 34, 42, 53] of related problems largely take the compressed sensing theory for granted and assume (explicitly or implicitly) either the incoherence or the restricted isometry property without proof.

Let us state the perhaps simplest criterion for exact recoverability of the incoherence approach.

Proposition 1. [17, 23] *BP reconstructs perfectly any target X of sparsity*

$$s \leq \frac{1}{2}\left(\frac{1}{\mu(\mathbf{\Phi})}+1\right) \tag{12}$$

where the sparsity $s = \|X\|_0$ is the number of nonzero components in X and the coherence parameter $\mu(\mathbf{\Phi})$ is defined as

$$\mu(\mathbf{\Phi}) = \max_{i\neq j} \frac{\left|\sum_l \Phi_{li}\Phi^*_{lj}\right|}{\sqrt{\sum_l |\Phi_{li}|^2 \sum_l |\Phi_{lj}|^2}}.$$

Proposition 1 implies that the lower the coherence of the sensing matrix is the more massive the exactly recoverable target can be. Under the condition (12), a simple greedy algorithm called Orthogonal Matching Pursuit (OMP) can provably find the minimizer of (11) in at most s iterations [48].

To construct sensing matrices of low coherence let us define the MIMO-sensor ensemble as follows. Let the incident angles $\theta_k, k = 1, ..., p$, be independently and identically distributed according to the probability density function $f^{\mathrm{i}} \in C^h([-\pi, \pi])$; for every incident angle let the sampling angles $\tilde{\theta}_l, l = 1, ..., n$, be independently and identically distributed according to the probability density function $f^{\mathrm{s}} \in C^h([-\pi, \pi])$ where $h > 0$ is the degree of smoothness. Define $\mathrm{supp}(f^{\mathrm{i}}) = \{\theta : f^{\mathrm{i}}(\theta) \neq 0\}$ and $\mathrm{supp}(f^{\mathrm{s}}) = \{\theta : f^{\mathrm{s}}(\theta) \neq 0\}$. We call $\theta_* \in [-\pi, \pi]$ a *Blind Spot* if there exists a pair $\mathbf{r}, \mathbf{r}' \in \mathcal{L}$ such that

$$\left|(\mathbf{r}-\mathbf{r}')\cdot(\cos\theta_*, \sin\theta_*)\right| = |\mathbf{r}-\mathbf{r}'|. \tag{13}$$

In other words, the set of Blind Spots consists of all the angles between the $x-$axis and $\mathbf{r}-\mathbf{r}', \forall \mathbf{r}, \mathbf{r}' \in \mathcal{L}$.

In Section 3, we prove that the following coherence bound for the sensing matrix with entries (10).

Theorem 1. *Let the sensing matrix $\mathbf{\Phi}$ be given according to the sensor ensemble. Suppose*

$$m \leq \frac{\delta}{8} e^{K^2/2}, \quad \delta, K > 0. \tag{14}$$

Then the sensing matrix (10) satisfies the coherence bound

$$\mu(\mathbf{\Phi}) < \left(\chi^{\mathrm{i}} + \frac{\sqrt{2}K}{\sqrt{p}}\right)\left(\chi^{\mathrm{s}} + \frac{\sqrt{2}K}{\sqrt{n}}\right) \tag{15}$$

with probability greater than $(1-\delta)^2$ where in general χ^{i} (resp. χ^{s}) satisfies the bound

$$\chi^{\mathrm{i}} \leq c_t(1+\omega\ell)^{-1/2}\|f^{\mathrm{i}}\|_{t,\infty}, \tag{16}$$

$$\textit{resp.} \quad \chi^{\mathrm{s}} \leq c_t(1+\omega\ell)^{-1/2}\|f^{\mathrm{s}}\|_{t,\infty}, \tag{17}$$

where $\|\cdot\|_{t,\infty}$ is the Hölder norm of order $t > 1/2$ and the constant c_t depends only on t. If, however, $\mathrm{supp}(f^{\mathrm{i}})$ (resp. $\mathrm{supp}(f^{\mathrm{s}})$) does not contains any Blind Spot, then χ^{i} (resp. χ^{s}) satisfies the bound

$$\chi^{\mathrm{i}} \leq c_h(1+\omega\ell)^{-h}\|f^{\mathrm{i}}\|_{h,\infty}, \tag{18}$$

$$\textit{resp.} \quad \chi^{\mathrm{s}} \leq c_h(1+\omega\ell)^{-h}\|f^{\mathrm{s}}\|_{h,\infty}, \quad \|f^{\mathrm{i}}\|_{h,\infty} = \sum_{|k|\leq h}\left\|\frac{d^k}{d\theta^k}f^{\mathrm{i}}\right\|_\infty \tag{19}$$

where the constant c_h depends only on h.

Remark 1. *Theorem 1 along with Proposition 1 then imply that any target of sparsity up to*

$$s \leq \frac{1}{2} + \frac{1}{2}\left(\chi^{\mathrm{i}} + \frac{\sqrt{2}K}{\sqrt{p}}\right)^{-1}\left(\chi^{\mathrm{s}} + \frac{\sqrt{2}K}{\sqrt{n}}\right)^{-1} \tag{20}$$

can be exactly recovered by BP.

If $\omega\ell$ is sufficiently large (which is the high frequency limit referred to in the title), the dominant term on the right hand side of (20) is

$$\frac{\sqrt{np}}{4K^2} \tag{21}$$

in view of (16)-(19).

Note that the high frequency limit for the Helmholtz equation is different from that for the Schrödigner equation. The high frequency quantum scattering is essentially linear (without the Born approximation) and can be solved by the Radon transform [35].

To improve the sparsity constraint (12), Tropp [50] develops an approach in which the recoverability is only probabilistic in the following ensemble of targets. Let the *target ensemble* consist of target vectors with at most s non-zero entries whose phases are independently uniformly distributed in $[0, 2\pi]$ and whose support indices are independently and randomly selected from the index set $\{1, 2, ..., m\}$.

The following theorem is a reformulation of results due to Tropp [50]. We refer the reader to [22] for the derivation of Proposition 2.

Proposition 2. *Assume the matrix $\mathbf{\Phi}$ has all unit columns. Let X be drawn from the target ensemble. Assume that*

$$\mu^2(\mathbf{\Phi})s \leq \left(8 \ln \frac{m}{\tau}\right)^{-1}, \quad \tau \in (0, 1) \tag{22}$$

and that for $q \geq 1$

$$3\left(\frac{q \ln s}{2 \ln \frac{m}{\tau}}\right)^{1/2} + \frac{s}{m}\|\mathbf{\Phi}\|_2^2 \leq \frac{1}{4e^{1/4}}. \tag{23}$$

Then X is the unique solution of BP with probability $1 - 2\tau - s^{-q}$. Here $\|\mathbf{\Phi}\|_2$ denotes the spectral norm of $\mathbf{\Phi}$.

Remark 2. *When the matrix $\mathbf{\Phi}$ has all unit elements, as in (10), the condition (23) becomes*

$$3\left(\frac{q \ln s}{2 \ln \frac{m}{\tau}}\right)^{1/2} + \frac{s}{m\rho}\|\mathbf{\Phi}\|_2^2 \leq \frac{1}{4e^{1/4}} \tag{24}$$

where $\rho = \#$rows in $\mathbf{\Phi}$.

Proposition 2 calls for the control of the spectral norm of $\mathbf{\Phi}$, in addition to $\mu(\mathbf{\Phi})$, in order to relax the sparsity constraint from (12) to (22).

In Section 4 we prove the following spectral norm bound.

Theorem 2. *Under the assumptions of Theorem 1 the matrix $\mathbf{\Phi}$ has full rank and its spectral norm satisfies the bound*

$$\|\mathbf{\Phi}\|_2^2 \leq 2m \tag{25}$$

with probability greater than

$$\left(1 - c_1\sqrt{\frac{np-1}{m}}\right)^{n(n-1)p(p-1)}, \quad n, p \geq 2 \tag{26}$$

for some constant $c_1 > 0$.

In the SIMO case $p = 1$ *we have*

$$\|\mathbf{\Phi}\|_2^2 \leq 2m \tag{27}$$

with probability larger than

$$\left(1 - c_1\sqrt{\frac{n-1}{m}}\right)^{n(n-1)}, \quad n \geq 2. \tag{28}$$

Remark 3. *The probability bounds (26) and (28) are probably far from being optimal. For* $np \ll m$, *a lower bound for (26) would be*

$$1 - c_1 n(n-1)p(p-1)\sqrt{\frac{np-1}{m}}$$

which requires $m \gg (np)^5$ *to be close to unity.*

When this is violated, we have to rely on Theorem 1 and Proposition 1 which together guarantees recovery with probability greater than $(1-\delta)^2$ *but with a higher sensor-to-target ratio.*

Now we are ready to prove the main result for inverse Born scattering.

Theorem 3. *Let the sensors and the target be drawn randomly from the sensor and target ensembles, respectively, and consider the sensing matrix* $\mathbf{\Phi}$ *of the entries defined by (9)-(10). If (14) holds, then the targets of sparsity up to*

$$s < \left(8\ln\frac{m}{\varepsilon}\right)^{-1}\left(\chi^{\mathrm{i}} + \frac{\sqrt{2}K}{\sqrt{p}}\right)^{-2}\left(\chi^{\mathrm{s}} + \frac{\sqrt{2}K}{\sqrt{n}}\right)^{-2} \tag{29}$$

can be recovered by BP with probability greater than

$$\left(\left(1 - c_1\sqrt{\frac{np-1}{m}}\right)^{n(n-1)p(p-1)} - 2\delta\right)\left(1 - 2\tau - s^{-q}\right), \quad n \geq 2, \quad p \geq 2 \tag{30}$$

for some constant $c_1 > 0$ *where, for* $pn \gg s$, q *can be chosen as*

$$q = \frac{\ln m - \ln\varepsilon}{72e^{1/2}\ln s}.$$

In the SIMO case the probability bound (30) becomes

$$\left(\left(1 - c_1\sqrt{\frac{n-1}{m}}\right)^{n(n-1)} - 2\delta\right)\left(1 - 2\tau - s^{-q}\right), \quad n \geq 2. \tag{31}$$

Remark 4. *Our results can be extended to the case that the sampling angles are not independent of the incident angles by adjusting the probability (26) (and hence (30) and (31)) in the spectral norm bound. An important example is the multistatic data matrix with* $\tilde{\theta}_j = -\theta_j, j = 1, ..., n$. *Such a setting is employed in the well known and widely used MIMO imaging scheme called MUSIC (standing for* MU*ltiple-*SI*gnal-*C*lassification) with* $p = n$ [12, 46] *(see the Conclusion).*

Previously in [22], *we have applied the compressed sensing methodology to imaging with the multistatic data matrix under the paraxial approximation and the assumption that the point scatterers lie on a transverse plane.*

Proof. First, the coherence estimate (15) and the sparsity constraint (29) implies (22).

Now the norm bound (25) implies (23) if

$$3\left(\frac{q\ln s}{2\ln\frac{m}{\tau}}\right)^{1/2}+\frac{2s}{np}\leq\frac{1}{4e^{1/4}},\quad q>1. \tag{32}$$

Hence for $np\gg s$ we can choose q in (23) to be

$$q=\frac{\ln m-\ln\tau}{72\sqrt{e}\ln s}.$$

Since Theorems 1 and 2 hold simultaneously with probability greater than

$$\left(1-c_1\sqrt{\frac{np-1}{m}}\right)^{n(n-1)p(p-1)}-2\delta,\quad p,n\geq 2$$

and since the target ensemble is independent of the sensor ensemble we have the bound (30) for the probability of exact recovery. The proof for the SIMO case is the same.

This completes the proof of Theorem 3.

□

2.2. **SIMO/MISO exact inverse scattering.** Next we turn to the exact inverse scattering (7)-(8) which takes into account all the multiple scattering effects. As the previous simulation shows [22], multiple scattering can severely degrade the performance of the imaging method based on the Born approximation.

Consider both the SIMO measurement with $p=1$ and the MISO measurement with $n=1$. Note that in the MISO measurement, various plane waves are incident upon the scatterers *one at a time* and the corresponding scattering amplitudes are sampled at a fixed direction. By the reciprocity of wave propagation in a time-invariant medium, reversing the incident and scattered waves and interchanging their roles leave the scattering amplitude unchanged,

$$A(\hat{\mathbf{r}},\mathbf{d})=A(-\mathbf{d},-\hat{\mathbf{r}})$$

(see Appendix A for a proof). Therefore, the SIMO and MISO cases are equivalent to each other.

Hereafter we will restrict our attention to the SIMO case. To this end, we will work with the alternative definition of the target vector $X=(\nu_j u(\mathbf{r}_j))\in\mathbb{C}^m$. The reason for this is that the problem then has the *appearance* of linear system

$$Y=\mathbf{\Phi}X \tag{33}$$

where the sensing matrix $\mathbf{\Phi}$ has the entries

$$\Phi_{lj}=e^{-i\omega(z_j\sin\tilde{\theta}_l+x_j\cos\tilde{\theta}_l)} \tag{34}$$

and is *independent* of the incident field. We then apply Theorem 3 with $p=1$ and sufficiently large n to recover X with high probability. To recover ν from X, we observe that as long as $u(\mathbf{r}_{i_j})\neq 0,\forall j$, the support of ν is the same as that of X. Indeed, the target strength $\nu=(\nu_j)\in\mathbb{C}^m$ can be recovered exactly by solving the system of nonlinear equations on the target support as follows.

Define the illumination and full field vectors at the locations of the scatterers:

$$\begin{aligned}U^{\mathrm{i}}&=(u^{\mathrm{i}}(\mathbf{r}_{i_1}),...,u^{\mathrm{i}}(\mathbf{r}_{i_s}))^T\in\mathbb{C}^s\\ U&=(u(\mathbf{r}_{i_1}),...,u(\mathbf{r}_{i_s}))^T\in\mathbb{C}^s.\end{aligned}$$

Let $\mathbf{G}$ be the $s\times s$ matrix

$$\mathbf{G}=[(1-\delta_{jl})G(\mathbf{r}_{i_j},\mathbf{r}_{i_l})]$$

and $\mathcal{V}$ the diagonal matrix

$$\mathcal{V} = \mathrm{diag}(\nu_{i_1}, ..., \nu_{i_s}).$$

The Foldy-Lax equation (8) can be written as

$$U = U^{\mathrm{i}} + \omega^2 \mathbf{G}\mathcal{V}U \tag{35}$$

from which we obtain

$$U = \left(\mathbf{I} - \omega^2 \mathbf{G}\mathcal{V}\right)^{-1} U^{\mathrm{i}} \tag{36}$$

and

$$X = \mathcal{V}U = \mathcal{V}\left(\mathbf{I} - \omega^2 \mathbf{G}\mathcal{V}\right)^{-1} U^{\mathrm{i}} \tag{37}$$

provided that ω^{-2} is not an eigenvalue of $\mathbf{G}\mathcal{V}$. The exciting field then determines the scattering amplitude by (7) which yields the (nonlinear) system

$$Y = \mathbf{\Phi}X = \mathbf{\Phi}\mathcal{V}\left(\mathbf{I} - \omega^2 \mathbf{G}\mathcal{V}\right)^{-1} U^{\mathrm{i}} \tag{38}$$

where the sensing matrix entries are given by (34).

Proposition 3. *Suppose*

$$\omega^{-2} \quad \textit{is not an eigenvalue of the matrix } \mathbf{G}\mathcal{V} \tag{39}$$

and

$$U^{\mathrm{i}} \quad \textit{is not orthogonal to any row vector of } \left(\mathbf{I} - \omega^2 \mathbf{G}\mathcal{V}\right)^{-1}. \tag{40}$$

Then the solution $\mathcal{V}$ of (37) is given by

$$\mathcal{V} = \mathrm{diag}\left[\frac{X}{\omega^2 \mathbf{G}X + U^{\mathrm{i}}}\right] \tag{41}$$

where the division is in the entry-wise sense (Hadamard product). In this case, $\mathrm{supp}(\mathcal{V}) = \mathrm{supp}(X)$.

Proof. Note that

$$\mathcal{V}\left(\mathbf{I} - \omega^2 \mathbf{G}\mathcal{V}\right)^{-1} = \left(\mathbf{I} - \omega^2 \mathcal{V}\mathbf{G}\right)^{-1} \mathcal{V}.$$

Hence eq. (37) can be written as

$$X = \left(\mathbf{I} - \omega^2 \mathcal{V}\mathbf{G}\right)^{-1} \mathcal{V}U^{\mathrm{i}}$$

or equivalently

$$\left(\mathbf{I} - \omega^2 \mathcal{V}\mathbf{G}\right) X = \mathcal{V}U^{\mathrm{i}}. \tag{42}$$

Solving (42) for the diagonal matrix $\mathcal{V}$ entry-by-entry, we obtain (41) which is well-defined if

$$\omega^2 \mathbf{G}X + U^{\mathrm{i}} \quad \text{contains no zero component.} \tag{43}$$

Since

$$\omega^2 \mathbf{G}X + U^{\mathrm{i}} = \left(\mathbf{I} - \omega^2 \mathbf{G}\mathcal{V}\right)^{-1} U^{\mathrm{i}} = U$$

(43) follows from (40).

□

Corollary 1. *Condition (43) holds and hence (41) is well-defined if*

$$\omega^2 \|\mathbf{G}\mathcal{V}\| < 1/2 \tag{44}$$

where $\|\cdot\|$ equals the maximum of the absolute row sums of the matrix corresponding to the operator norm on L^∞.

Proof. Clearly $U^{\mathrm{i}} + \omega^2 \mathbf{G} X$ contains no zero entry if

$$\omega^2 \|\mathbf{G} X\| < 1 \tag{45}$$

since every component of U^{i} has modulus one. As

$$\|\mathbf{G} X\| = \|\mathbf{G}\mathcal{V} \left(\mathbf{I} - \omega^2 \mathbf{G}\mathcal{V}\right)^{-1} \|$$

(45) follows from (44). □

Theorem 4. *Suppose $p = 1$, (14), (39) and (40) hold. Let X be a BP solution for the system (33) with the matrix entries (34) according to Theorem 3. The formula (41) recovers exactly the target of sparsity*

$$s < \left(8 \ln \frac{m}{\varepsilon}\right)^{-1} \left(\chi^{\mathrm{s}} + \frac{\sqrt{2} K}{\sqrt{n}}\right)^{-2} \tag{46}$$

with probability at least as in (31) and χ^{s} satisfies the bound (17) or (19) depending on whether $\mathrm{supp}(f^{\mathrm{s}})$ *contains a Blind Spot or not.*

Remark 5. *The resonance frequency violating (39) is related to the transmission eigenvalue for continuous media where an analogous non-resonance condition is also needed to ensure the existence and uniqueness of the solution to the inverse scattering problem* [13, 37].

If 1 *is an eigenvalue of $\omega^2 \mathbf{G}\mathcal{V}$, the existence of solution for (35) requires that U^{i} be orthogonal to the eigenspace of $\omega^2 \mathbf{G}\mathcal{V}$ corresponding to* 1. *Then other physical constraints (such as the minimum energy solution) need to be taken into account in order to obtain a unique solution.*

The simplest example for resonance is this: Two point scatterers have the strengths ν_{i_1}, ν_{i_2} such that $\mathrm{sign}(\nu_{i_1}) = \mathrm{sign}(\nu_{i_2}) = \mathrm{sign}(G^*(\mathbf{r}_{i_1}, \mathbf{r}_{i_2}))$. *Then*

$$\mathbf{G}\mathcal{V} = \begin{bmatrix} 0 & |\nu_{i_1} G(\mathbf{r}_{i_1}, \mathbf{r}_{i_2})| \\ |\nu_{i_2} G(\mathbf{r}_{i_1}, \mathbf{r}_{i_2})| & 0 \end{bmatrix}$$

is real and symmetric and has the positive eigenvalue $\sqrt{|\nu_{i_1}\nu_{i_2}|}|G(\mathbf{r}_{i_1}, \mathbf{r}_{i_2})|$. The resonance frequency is $|\nu_{i_1}\nu_{i_2}|^{-1/4}|G(\mathbf{r}_{i_1}, \mathbf{r}_{i_2})|^{-1/2}$ in this case.

Remark 6. *In view of (36), (40) means that U has no zero component. In other words, the target is not shadowed by itself in any way.*

Since the negation of (40) is an algebraic constraint, (40) are satisfied almost surely in the target ensemble under (39).

2.3. **Stability w.r.t. errors.** Here we consider the situation where the measurement or model errors are present. In the former case, the data may be contaminated by noise. In the latter case, the errors may be due to, for instance, the fact that the targets are slightly off the grid. In this case the target vector X does not represent the true targets exactly due to model mismatch and is only the best approximation given the model. In either case, the data vector can be written as

$$Y = \mathbf{\Phi} X + E \tag{47}$$

where E represents the errors. In the case of measurement noise, E is independent of the targets while in the case of model mismatch, E depends explicitly on the targets.

Since $A(\hat{\mathbf{r}}, \mathbf{d})$ is an analytic function of both $\hat{\mathbf{r}}$ and $\mathbf{d}$ and hence for the given noisy data, in general no solution exists to the inverse scattering problem. Even if a solution does exist, it does not depend continuously on the measured data in any reasonable norm.

To deal with the problem of ill-posedness we consider, instead of the Tikhonov regularization, the L^1-regularization

$$\min_Z \frac{1}{2}\|Y - \mathbf{\Phi} Z\|_2^2 + \lambda \|Z\|_1 \tag{48}$$

where λ is the Lagrangian multiplier to be given below. This is the Lagrangian form of the basis pursuit denoising (BPDN) [3, 11] and the *lasso* in the statistics literature [47, 19]. Let $\hat{X}$ be the minimizer of (48).

The starting point of our analysis is the following result, due to Tropp [49], concerning the error bound and the recoverability of the target support in the presence of noise.

Proposition 4. [49] *Assume that $\mathbf{\Phi}$ has all unit columns and that $\|E\|_2 \le \varepsilon$.*

Suppose $\mu(\mathbf{\Phi})s \le 1/3$. Then the minimizer $\hat{X}$ of (48) with $\lambda = 2\varepsilon$ is unique and its support is contained in $\mathrm{supp}(X)$*. Moreover,*

$$\|\hat{X} - X\|_\infty \le \left(3 + \sqrt{3/2}\right)\varepsilon. \tag{49}$$

Remark 7. *When the matrix $\mathbf{\Phi}$ has all unit entries, as in (34), and the error term satisfies $\|E\|_2 \le n^{1/2}\varepsilon$, then (49) holds with $\lambda = 2n\varepsilon$.*

Define the reconstruction of $\mathcal{V}$ to be

$$\hat{\mathcal{V}} = \mathrm{diag}\left[\frac{\hat{X}}{U^{\mathrm{i}} + \omega^2 \mathbf{G}\hat{X}}\right] \tag{50}$$

in analogy to (41).

Using Proposition 4 we derive an error bound and a sufficient condition under which the support of the reconstruction is exactly the same as the original.

Theorem 5. *Suppose $\|E\|_2 \le \varepsilon n^{1/2}$ and let $\hat{X}$ be the solution to (48) with $\lambda = 2\varepsilon n$. Assume*

$$\mu(\mathbf{\Phi})s \le 1/3 \tag{51}$$

and

$$\omega^2\|\mathbf{G}\mathcal{V}\| < \frac{1 - (3+\sqrt{3/2})\varepsilon\|\mathbf{G}\|}{2 - (3+\sqrt{3/2})\varepsilon\|\mathbf{G}\|} \ \left(< \frac{1}{2}\right). \tag{52}$$

Then (50) is well-defined and satisfies the error bound:

$$\|\mathcal{V} - \hat{\mathcal{V}}\| \le \frac{2\left(1 + \omega^2\|\mathbf{G}\|\|\mathcal{V}\|\right)(3+\sqrt{3/2})\varepsilon}{b_0(b_0 - \omega^2(3+\sqrt{3/2})\varepsilon\|\mathbf{G}\|)}, \quad b_0 \equiv \frac{1 - 2\omega^2\|\mathbf{G}\mathcal{V}\|}{1 - \omega^2\|\mathbf{G}\mathcal{V}\|}. \tag{53}$$

Moreover, $\mathrm{supp}(\hat{\mathcal{V}}) = \mathrm{supp}(\hat{X}) \subset \mathrm{supp}(X)$*. On the other hand, if*

$$\omega^2\|\mathbf{G}\mathcal{V}\| \ < \ \frac{1 - (3+\sqrt{3/2})\varepsilon\|\mathcal{V}^{-1}\|}{2 - (3+\sqrt{3/2})\varepsilon\|\mathcal{V}^{-1}\|} \tag{54}$$

then $\mathrm{supp}(\hat{X}) = \mathrm{supp}(X)$*. Therefore under (52) and (54),* $\mathrm{supp}(\hat{\mathcal{V}}) = \mathrm{supp}(\mathcal{V})$*, i.e. the support of the target is perfectly recovered.*

The proof of Theorem 5 is given in Section 5.

Remark 8. *Condition (51) is slightly stronger than (12) and hence the OMP algorithm can be used to solve (48)* [49]*.*

Condition (52), (54) and (44) all say in various ways that the scatterers are either weak or far apart.

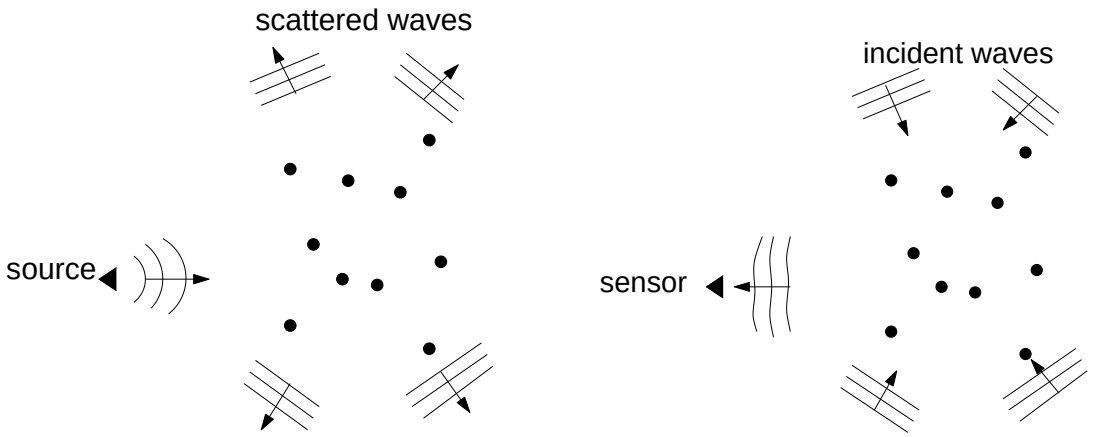

FIGURE 2. SIMO (left) and MISO (right) measurements with single point source (left) and single point sensor (right), respectively.

2.4. **Three dimensions.** Here we consider the extension of the coherence bound, Theorem 1, to the three dimensional setting. The main point here is to demonstrate the decoherence effect due to the extra dimension. For simplicity, we will not consider the improved performance as a result of avoiding Blind Spots.

Instead of a square lattice, the computational domain is a cubic lattice of spacing ℓ. Each side of the cubic lattice has $m^{1/3}$ grid points. In three dimensions, the scattering amplitude has the same expression (7), except that the sampling direction $\hat{\mathbf{r}} = (\tilde{\alpha}, \tilde{\beta}, \tilde{\gamma})$ are parametrized by two polar angles $\tilde{\theta}, \tilde{\phi}$ as

$$\tilde{\alpha} = \cos\tilde{\theta}\cos\tilde{\phi}, \quad \tilde{\beta} = \cos\tilde{\theta}\sin\tilde{\phi}, \quad \tilde{\gamma} = \sin\tilde{\theta} \tag{55}$$

Theorem 6. *Let the sensing matrix $\mathbf{\Phi}$ be given according to the sensor ensemble. Suppose (14) holds for some constants δ and K and suppose $f^{\mathrm{i}}, f^{\mathrm{s}} \in C^1$. Then the sensing matrix (10) satisfies the coherence bound*

$$\mu(\mathbf{\Phi}) < \left(\chi^{\mathrm{i}} + \frac{\sqrt{2}K}{\sqrt{p}}\right)\left(\chi^{\mathrm{s}} + \frac{\sqrt{2}K}{\sqrt{n}}\right) \tag{56}$$

with probability greater than $(1-\delta)^2$ where in general χ^{i} (resp. χ^{s}) satisfies the bound

$$\chi^{\mathrm{i}} \le c(1+\omega\ell)^{-1}\|f^{\mathrm{i}}\|_{1,\infty} \quad \big(\textit{resp.} \quad \chi^{\mathrm{s}} \le c(1+\omega\ell)^{-1}\|f^{\mathrm{i}}\|_{1,\infty}\big)\,. \tag{57}$$

Consequently, the asymptotic behavior (21) sets in faster in three dimensions than in two dimension in general.

2.5. **Diffraction tomography: point sensors or sources.** Instead of measuring the scattering amplitudes, one could measure the scattered field at a set of sampling points and reconstruct the targets from the measurement data. Likewise the incident wave may be a spherical wave emitted from a point source instead of a plane wave from far field. This is the measurement with point sources or sensors. We will focus on the SIMO/MISO settings and discuss both the two and three dimensional cases.

First consider the simple setting with one point sensor at a fixed location measuring the scattered fields due to multiple incident plane waves (Figure 2, right) emitted one at a time. This is a MISO measurement with one fixed point sensor. By the input-output reciprocity (Appendix A), this is

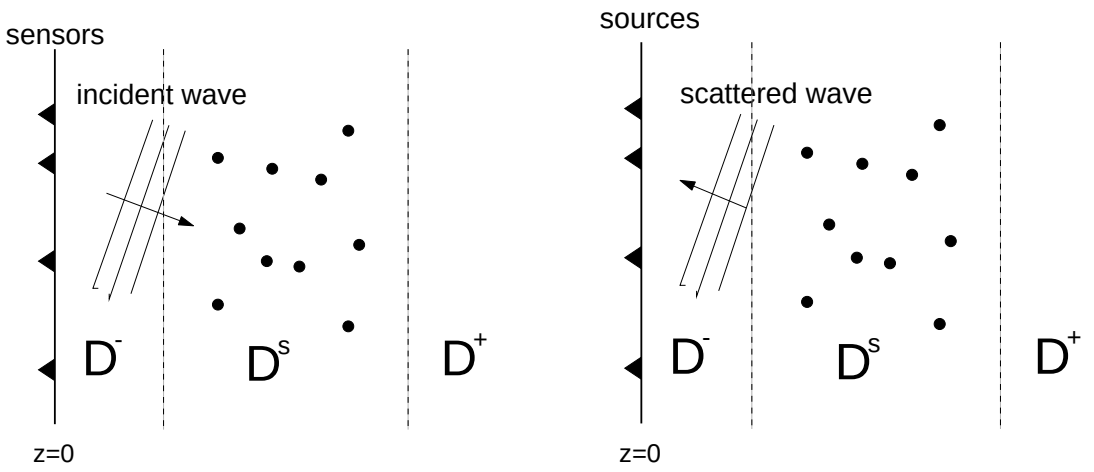

FIGURE 3. SIMO (left) and MISO (right) measurements with single incident plane wave (left) and single sampling direction (right), respectively.

equivalent to the SIMO measurement of measuring multiple scattering amplitudes due to one point source in near field (Figure 2, left). Hence it suffices to analyze the SIMO case.

Analogous to (7), the scattering amplitude in the direction $\hat{\mathbf{r}}$ is given by

$$A(\hat{\mathbf{r}}, u^{\mathrm{i}}) = \frac{\omega^2}{4\pi} \sum_{j=1}^{m} \mathcal{G}(\mathbf{r}_j, \mathbf{r}_0) \nu_j e^{-i\omega \mathbf{r}_j \cdot \hat{\mathbf{r}}}, \quad u^{\mathrm{i}}(\mathbf{r}) = G(\mathbf{r}, \mathbf{r}_0) \tag{58}$$

where $\mathcal{G}$ is the Green function including the multiple scattering effects, i.e.

$$\mathcal{G}(\mathbf{r}, \mathbf{r}_0) = G(\mathbf{r}, \mathbf{r}_0) + \omega^2 \sum_{j=1}^{m} \nu_j \mathcal{G}(\mathbf{r}_j, \mathbf{r}_0) G(\mathbf{r}, \mathbf{r}_j), \quad \mathbf{r} \neq \mathbf{r}_k, \ k = 0, ..., s \tag{59}$$

$$\mathcal{G}(\mathbf{r}_k, \mathbf{r}_0) = G(\mathbf{r}_k, \mathbf{r}_0) + \omega^2 \sum_{j \neq k} \nu_j \mathcal{G}(\mathbf{r}_j, \mathbf{r}_0) G(\mathbf{r}_k, \mathbf{r}_j), \ k = 1, ..., s \tag{60}$$

analogous to the Foldy-Lax equation (8). Define the target vector $X = (X_j) \in \mathbb{C}^m$

$$X_j = \mathcal{G}(\mathbf{r}_j, \mathbf{r}_0) \nu_j,$$

the data vector $Y = (Y_k) \in \mathbb{C}^n$

$$Y_k = \frac{4\pi}{\omega^2} A(\hat{\mathbf{r}}_k)$$

where $\hat{\mathbf{r}}_k = (\cos\tilde{\theta}_k, \sin\tilde{\theta}_k), k = 1, ..., n$ are the incident directions. Then we have $Y = \mathbf{\Phi} X$ where the sensing matrix $\mathbf{\Phi} = [\Phi_{kj}]$ is exactly as in (34).

We can solve this problem exactly as in Section 2.2 by first finding X and then setting

$$\begin{aligned} \nu_j &= \frac{X_j}{\mathcal{G}(\mathbf{r}_j, \mathbf{r}_0)} \\ &= \frac{X_j}{G(\mathbf{r}_j, \mathbf{r}_0) + \omega^2 \sum_{l=1}^{m} X_l G(\mathbf{r}_0, \mathbf{r}_l)} \end{aligned}$$

where we have used (59). In the noisy case (47), we proceed as before and set

$$\nu_j = \frac{\hat{X}_j}{G(\mathbf{r}_j, \mathbf{r}_0) + \omega^2 \sum_{l=1}^{m} \hat{X}_l G(\mathbf{r}_0, \mathbf{r}_l)}.$$

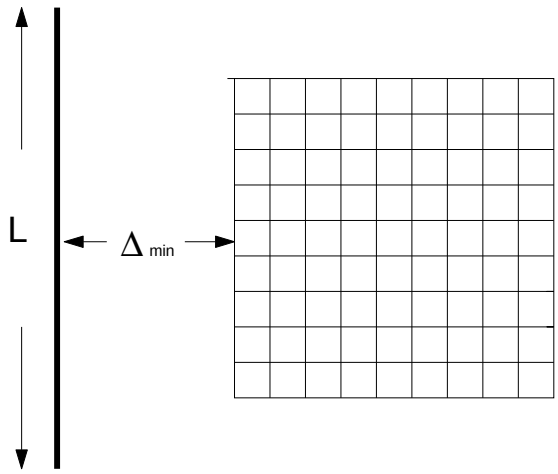

FIGURE 4. Near-field imaging geometry

In other words, Theorems 4 and 5 can be immediately generalized to this setting (one point source or one point sensor).

Next let us turn to the more complicated measurement with multiple point sources and one sampling direction (MISO, Figure 3, right) or one incident wave and multiple sensors (SIMO, Figure 3, left). By the input-output reciprocity (Appendix A), the two settings are equivalent to each other. So we focus on the SIMO case below which requires similar but more delicate estimates than before.

We are primarily interested in the imaging set-up called *diffraction tomography* [1]. First, assume the two dimensional setting with the z-axis as the imaging direction (see Figure 3). To describe the near field measurement we need the Green function for (1)

$$G(\mathbf{r}) = \frac{-i}{4} H_0^{(1)}(\omega|\mathbf{r}|)$$

where $H_0^{(1)}$ is the zeroth order Hankel function of the first kind and admits the Sommerfeld integral representation

$$H_0^{(1)}(\omega|\mathbf{r}|) = \frac{1}{\pi} \int e^{i\omega(|z|\gamma(\alpha)+x\alpha)} \frac{d\alpha}{\gamma(\alpha)} \tag{61}$$

with

$$\gamma(\alpha) = \begin{cases} \sqrt{1-\alpha^2}, & |\alpha| < 1 \\ i\sqrt{\alpha^2-1}, & |\alpha| > 1 \end{cases}$$

[1].

As shown in Figure 3 the whole space is divided into three domains $D^- \cup D^{\mathrm{s}} \cup D^+$ where the infinite slab D^{s} contains all the scatterers and D^-, D^+ are free half spaces. The sensors are placed in either D^- (the reflection mode) or D^+ (the transmission mode).

To fixed the idea, suppose the sensors are located in the line segment of length L on $\{z = 0\} \subset D^-$ symmetrical w.r.t. to the square lattice of the computational domain, see Figure 4. Let $\Delta_{\min}$ and $\Delta_{\max}$, respectively, be the minimum and maximum distances between the line segment and the lattice. In two dimensions,

$$\Delta_{\max} = \sqrt{\frac{1}{4}(L + \ell\sqrt{m})^2 + (\Delta_{\min} + \ell\sqrt{m})^2}. \tag{62}$$

Using (61) we can express the scattered field in $D^- \cup D^+$ as

$$u^{\rm s}(\mathbf{r}) = \frac{-i\omega^2}{4\pi}\int_{D^{\rm s}} d\mathbf{r}' \int \frac{d\alpha}{\beta}\nu(\mathbf{r}')u(\mathbf{r}')e^{i\omega(\beta|z-z'|+\alpha(x-x'))}, \quad \mathbf{r}\in D^-\cup D^+. \tag{63}$$

Let $\mathbf{a}_j = (\xi_j, 0), j = 1, ..., n$ where ξ_j are i.i.d. uniform r.v.s in a square of length L. Let $Y = (u^{\rm s}(\mathbf{a}_j)) \in \mathbb{C}^n$ be the data vector. For the SIMO measurement at near field the sensing matrix elements, after factoring out ω^2, are simply

$$G(\mathbf{a}_j - \mathbf{r}_l) = \frac{-i}{4\pi}\int \frac{d\alpha}{\gamma} e^{i\omega(\gamma z_l + \alpha(\xi_j - x_l))}, \quad j = 1, ..., n,\ l = 1, ..., m.$$

For the three dimensional case, we use the Weyl representation formula for the Green function

$$-\frac{e^{i\omega|\mathbf{r}|}}{4\pi|\mathbf{r}|} = \frac{-i\omega}{8\pi^2}\int \frac{d\alpha d\beta}{\gamma} e^{[i\omega(\alpha x+\beta y+\gamma|z|)]} \tag{64}$$

where

$$\begin{aligned}\gamma &= \sqrt{1-\alpha^2-\beta^2}, \quad \alpha^2+\beta^2 \le 1\\ \gamma &= i\sqrt{\alpha^2+\beta^2-1}, \quad \alpha^2+\beta^2 > 1,\end{aligned}$$

[1].

Using (64) we can express the scattered field at $z = 0$ as

$$u^{\rm s}(\mathbf{r}) = -\frac{i\omega^3}{8\pi^2}\int_{D^{\rm s}} d\mathbf{r}' \int \frac{d\alpha d\beta}{\gamma}\nu(\mathbf{r}')u(\mathbf{r}')e^{i\omega(\gamma z' + \alpha(x-x') + \beta(y-y'))}, \quad \mathbf{r}\in D^-\cup D^+.$$

Let $\mathbf{a}_j = (\xi_j, \eta_j, 0), j = 1, ..., n$ where (ξ_j, η_j) are i.i.d. uniform r.v.s in a square of length L. Assume again that the square aperture is symmetrical w.r.t. the cubic lattice of the computational domain as indicated in Figure 4. For this imaging geometry, the maximum distance $\Delta_{\max}$ between the aperture and the lattice is

$$\Delta_{\max} = \sqrt{\frac{1}{4}(L+\ell m^{1/3})^2 + \frac{1}{4}(L+\ell m^{1/3})^2 + (\Delta_{\min}+\ell m^{1/3})^2}. \tag{65}$$

Let $Y = (u^{\rm s}(\mathbf{a}_j)) \in \mathbb{C}^n$ be the data vector. The SIMO sensing matrix elements , after factoring out ω^2, become

$$G(\mathbf{a}_j - \mathbf{r}_l) = \frac{-i\omega}{8\pi^2}\int \frac{d\alpha d\beta}{\gamma} e^{i\omega(\gamma z_l + \alpha(\xi_j - x_l) + \beta(\eta_j - y_l))}$$

for $j = 1, ..., n,\ l = 1, ..., m$.

Theorem 7. *Suppose*

$$m \le \frac{\delta}{2}e^{2K^2/r_0^2}, \quad \delta > 0 \tag{66}$$

where c_0 depends on the minimum distance $\Delta_{\min}$ between $\{z = 0\}$ and the lattice (For $d = 2$, $r_0 = \mathcal{O}(-\log\Delta_{\min})$; for $d = 3$, $r_0 = \mathcal{O}(\Delta_{\min}^{-1})$).

The mutual coherence obeys

$$\mu(\mathbf{\Phi}) \le |G(\Delta_{\max})|^{-2}\left(\frac{\sqrt{2}K}{\sqrt{n}} + \frac{c}{\sqrt{\omega L}}\right), \quad d = 2 \tag{67}$$

$$\mu(\mathbf{\Phi}) \le |G(\Delta_{\max})|^{-2}\left(\frac{\sqrt{2}K}{\sqrt{n}} + \frac{c}{\omega L}\right), \quad d = 3 \tag{68}$$

for some constant c (independent of $\omega > 0$ for $d = 2$ and $\omega > 1$ for $d = 3$), with probability greater than $(1-\delta)^2$, where $\Delta_{\max}$ is given by (62) for $d = 2$ and (65) for $d = 3$.

Remark 9. *In view of the presence of the factor* $|G(\Delta_{\max})|^{-2}$*, we see that Theorem 7 is useful primarily in the high frequency limit* $\omega \gg 1$ *with* $L = \mathcal{O}(1)$*.*

Analogous to Theorems 4 and 5, we have

Corollary 2. *In the absence of noise (*$\varepsilon = 0$*), let* X *be a BP solution with the sensing matrix of diffraction tomography. Under the same assumptions of Theorem 7 the formula (41) recovers exactly the target of sparsity smaller than*

$$\frac{1}{2}\left(1 + |G(\Delta_{\max})|^2 \left(\frac{\sqrt{2}K}{\sqrt{n}} + \frac{c}{\sqrt{\omega L}}\right)^{-1}\right), \qquad d = 2 \tag{69}$$

$$\frac{1}{2}\left(1 + |G(\Delta_{\max})|^2 \left(\frac{\sqrt{2}K}{\sqrt{n}} + \frac{c}{\omega L}\right)^{-1}\right), \qquad d = 3 \tag{70}$$

for some constant c *(independent of* $\omega > 0$ *for* $d = 2$ *and* $\omega > 1$ *for* $d = 3$*) with probability greater than* $(1-\delta)^2$*.*

In the presence of noise, Theorem 5 holds.

3. Proof of Theorem 1: Coherence bound

Proof. Denote $\hat{\mathbf{r}}_j = (\cos\tilde{\theta}_j, \sin\tilde{\theta}_j), \mathbf{d}_k = (\cos\theta_k, \sin\theta_k)$.

The pairwise coherence has the form

$$\frac{1}{pn}\left|\sum_{k=1}^{p} e^{i\omega \mathbf{d}_k\cdot(\mathbf{r}-\mathbf{r}')} \cdot \sum_{j=1}^{n} e^{i\omega \hat{\mathbf{r}}_j\cdot(\mathbf{r}-\mathbf{r}')}\right| \tag{71}$$

where $\mathbf{r}, \mathbf{r}'$ are two distinct points in the lattice $\mathcal{L}$. Note that the two summations in (71) are of the same type.

Consider the first summation over $k = 1, ..., p$. Let

$$P_k = \cos(\omega \mathbf{d}_k \cdot (\mathbf{r} - \mathbf{r}')), \quad Q_k = \sin(\omega \mathbf{d}_k \cdot (\mathbf{r} - \mathbf{r}'))$$

and

$$S_p = \sum_{k=1}^{p} P_k, \quad T_p = \sum_{k=1}^{p} Q_k.$$

Then the summation can be bounded by

$$\left|\sum_{k=1}^{p} e^{i\omega \mathbf{d}_k\cdot(\mathbf{r}-\mathbf{r}')}\right| \le \sqrt{|S_p - \mathbb{E}S_p|^2 + |T_p - \mathbb{E}T_p|^2} + \sqrt{|\mathbb{E}S_p|^2 + |\mathbb{E}T_p|^2} \tag{72}$$

We recall the Hoeffding inequality [26].

Proposition 5. *Let* $P_1, ..., P_p$ *be independent random variables. Assume that* $P_l \in [a_l, b_l], l = 1, ..., p$ *almost surely. Then we have*

$$\mathbb{P}\left[|S_p - \mathbb{E}S_p| \ge pt\right] \le 2\exp\left[-\frac{2p^2t^2}{\sum_{l=1}^{p}(b_l - a_l)^2}\right] \tag{73}$$

for all positive values of t*.*

We apply the Hoeffding inequality to both S_p and T_p. To this end, we have $b_l - a_l = 2, \forall l = 1, ..., p$. Set

$$t = K/\sqrt{p}, \quad K > 0.$$

Then we obtain

$$\mathbb{P}\left[p^{-1}\left|S_p - \mathbb{E}S_p\right| \geq K/\sqrt{p}\right] \leq 2e^{-K^2/2} \tag{74}$$

$$\mathbb{P}\left[p^{-1}\left|T_p - \mathbb{E}T_p\right| \geq K/\sqrt{p}\right] \leq 2e^{-K^2/2}. \tag{75}$$

Note that the quantities S_p, T_p depend on $\mathbf{r}-\mathbf{r}' = (x_i - x_j, z_i - z_j)$ but they possess the symmetry: $S_p(\mathbf{r}-\mathbf{r}') = S_p(\mathbf{r}'-\mathbf{r}), T_p(\mathbf{r}-\mathbf{r}') = -T_p(\mathbf{r}'-\mathbf{r})$. Furthermore, a moment of reflection reveals that thanks to the square symmetry of the lattice there are at most $m-1$ different values $|S_p|$ and $|T_p|$ among the $m(m-1)/2$ pairs of $(\mathbf{r}, \mathbf{r}')$.

We use (74)-(75) and the union bound to obtain

$$\mathbb{P}\left[\max_{i\neq j} p^{-1}\left|S_p - \mathbb{E}S_p\right| \geq K/\sqrt{p}\right] \leq 2(m-1)\cdot e^{-K^2/2}$$

$$\mathbb{P}\left[\max_{i\neq j} p^{-1}\left|T_p - \mathbb{E}T_p\right| \geq K/\sqrt{p}\right] \leq 2(m-1)\cdot e^{-K^2/2}$$

where the factor $4m$ is due to the structure of square lattice.

Hence, by (72)

$$\mathbb{P}\left[\max_{i\neq j} p^{-1}\left|\sum_{k=1}^{p} e^{i\omega\mathbf{d}_k\cdot(\mathbf{r}-\mathbf{r}')} - \mathbb{E}\left[\sum_{k=1}^{p} e^{i\omega\mathbf{d}_k\cdot(\mathbf{r}-\mathbf{r}')}\right]\right| < \sqrt{2}K/\sqrt{p}\right] > (1-2(m-1)e^{-K^2/2})^2. \tag{76}$$

Similarly we have for the second summation in (71)

$$\mathbb{P}\left[\max_{i\neq j} n^{-1}\left|\sum_{j=1}^{n} e^{i\omega\hat{\mathbf{r}}_j\cdot(\mathbf{r}-\mathbf{r}')} - \mathbb{E}\left[\sum_{j=1}^{n} e^{i\omega\hat{\mathbf{r}}_j\cdot(\mathbf{r}-\mathbf{r}')}\right]\right| < \sqrt{2}K/\sqrt{n}\right] > \left(1-2(m-1)e^{-K^2/2}\right)^2. \tag{77}$$

By (14) the right hand side of (76)-(77) is greater than $(1-\delta)^2$.

Consider $\mathbb{E}\left[\sum_{k=1}^{p} e^{i\omega\mathbf{d}_k\cdot(\mathbf{r}-\mathbf{r}')}\right]$. The same analysis below applies equally well to $\mathbb{E}\left[\sum_{j=1}^{n} e^{i\omega\hat{\mathbf{r}}_j\cdot(\mathbf{r}-\mathbf{r}')}\right]$.

If f^{i} is the uniform distribution over $[-\pi, \pi]$ or $[-\pi/2, \pi/2]$ then

$$\mathbb{E}\left[\sum_{k=1}^{p} e^{i\omega\mathbf{d}_k\cdot(\mathbf{r}-\mathbf{r}')}\right] = pJ_0(\omega|\mathbf{r}-\mathbf{r}'|)$$

where J_0 is the zeroth order Bessel function. In general, the exact expression is not available but we are concerned only with the asymptotic for $\omega|\mathbf{r}-\mathbf{r}'| \gg 1$.

The Bessel function has the asymptotic

$$J_0(\omega r) = \sqrt{\frac{2}{\pi\omega r}}\left\{\cos\left(\omega r - \pi/4\right) + \mathcal{O}((\omega r)^{-1})\right\}, \quad \omega r \gg 1. \tag{78}$$

That is, for $\omega\ell \gg 1$ there exists a constant $c > 0$ such that

$$J_0(\omega|\mathbf{r}-\mathbf{r}'|) < \frac{c}{\sqrt{\omega\ell}}, \quad \forall \mathbf{r}, \mathbf{r}' \in \mathcal{L}, \quad \mathbf{r} \neq \mathbf{r}' \tag{79}$$

In general,

$$\frac{1}{p}\mathbb{E}\left[\sum_{k=1}^{p} e^{i\omega\mathbf{d}_k\cdot(\mathbf{r}-\mathbf{r}')}\right] = \int_0^{2\pi} e^{i\omega\mathbf{d}\cdot(\mathbf{r}-\mathbf{r}')} f^{\mathrm{i}}(\theta)d\theta, \quad \mathbf{d} = (\cos\theta, \sin\theta) \tag{80}$$

which is the Herglotz wave function with kernel f^{i} in two dimensions. By assumption on f^{i} (80) is a finite sum of integrals of the form

$$\int_a^b e^{i\omega \mathbf{d}\cdot(\mathbf{r}-\mathbf{r}')} f^{\mathrm{i}}(\theta) d\theta \tag{81}$$

with $f^{\mathrm{i}} \neq 0$ in (a,b) whose asymptotic for $\omega\ell \gg 1$ can be analyzed by the method of stationary phase (Theorem XI. 14 and XI. 15 of [44]).

Proposition 6. *Let $g_{\mathbf{r},\mathbf{r}'}(\theta) = \mathbf{d}\cdot(\mathbf{r}-\mathbf{r}')/|\mathbf{r}-\mathbf{r}'|$ which is in $C^\infty([-\pi,\pi]), \forall \mathbf{r},\mathbf{r}' \in \mathcal{L}$.*

(i) Suppose $\frac{d}{d\theta} g_{\mathbf{r},\mathbf{r}'}(\theta) \neq 0, \forall \theta \in [a,b], \forall \mathbf{r},\mathbf{r}' \in \mathcal{L}$. Then for all $f^{\mathrm{i}} \in C_0^h([a,b])$

$$\left| \int e^{i\omega|\mathbf{r}-\mathbf{r}'| g_{\mathbf{r},\mathbf{r}'}(\theta)} f^{\mathrm{i}}(\theta) d\theta \right| \leq c_h (1+\omega|\mathbf{r}-\mathbf{r}'|)^{-h} \|f^{\mathrm{i}}\|_{h,\infty} \tag{82}$$

for some constant c_h independent of f^{i}. Moreover, since $\{g_{\mathbf{r},\mathbf{r}'} : \mathbf{r},\mathbf{r}' \in \mathcal{L}\}$ is a compact subset of $C^{h+1}([a,b])$, the constant c_h can be chosen uniformly for all $\mathbf{r},\mathbf{r}' \in \mathcal{L}$.

(ii) Suppose $\frac{d}{d\theta} g_{\mathbf{r},\mathbf{r}'}(\theta)$ vanishes at $\theta_* \in (a,b)$. Since $\frac{d^2}{d\theta^2} g_{\mathbf{r},\mathbf{r}'}(\theta_*) \neq 0$, there exists a constant $c_t, t > 1/2$ such that

$$\left| \int e^{i\omega|\mathbf{r}-\mathbf{r}'| g_{\mathbf{r},\mathbf{r}'}(\theta)} f^{\mathrm{i}}(\theta) d\theta \right| \leq c_t (1+\omega|\mathbf{r}-\mathbf{r}'|)^{-1/2} \|f^{\mathrm{i}}\|_{t,\infty} \tag{83}$$

where the constant c_t is independent of $\mathbf{r},\mathbf{r}' \in \mathcal{L}$.

Note that the condition

$$\frac{d}{d\theta} g_{\mathbf{r},\mathbf{r}'}(\theta) \neq 0, \quad \theta \in [a,b], \quad \forall \mathbf{r},\mathbf{r}' \in \mathcal{L}$$

is the same as saying that (a,b) does not contain any Blind Spot. Combining the estimates for

$$\chi^{\mathrm{i}} = \left| \int \left[e^{i\omega \mathbf{d}\cdot(\mathbf{r}-\mathbf{r}')} \right] f^{\mathrm{i}}(\theta) d\theta \right|, \quad \chi^{\mathrm{s}} = \left| \int \left[e^{i\omega \tilde{\mathbf{d}}\cdot(\mathbf{r}-\mathbf{r}')} \right] f^{\mathrm{s}} d\tilde{\theta} \right|,$$

using (76)-(77) and the identity

$$UV = (U-\bar{U})(V-\bar{V}) + \bar{U}(V-\bar{V}) + \bar{V}(U-\bar{U}) + \bar{U}\bar{V}$$

we obtain (15) with probability greater than $(1-\delta)^2$.

□

4. Proof of Theorem 2: Spectral norm bound

Proof. For the proof, it suffices to show that the matrix $\mathbf{\Phi}$ satisfies

$$\| \frac{1}{m} \mathbf{\Phi}\mathbf{\Phi}^* - \mathbf{I}_{np} \|_2 < 1 \tag{84}$$

where $\mathbf{I}_{np}$ is the $np \times np$ identity matrix with the corresponding probability bound (26). By the Gershgorin circle theorem, (84) would in turn follow from

$$\mu(\mathbf{\Phi}^*) < \frac{1}{np-1} \tag{85}$$

since the diagonal elements of $\mathbf{\Phi}\mathbf{\Phi}^*/m$ are unity.

The pairwise coherence amounts to calculating the expression

$$\frac{np}{m} \left| \sum_{l=1}^m \Phi_{jl} \Phi_{li}^* \right| = \frac{1}{m} \left| \sum_{l=1}^m e^{-i\omega(z_l \sin\theta + x_l \cos\theta)} e^{i\omega(z_l \sin\theta' + x_l \cos\theta')} e^{i\omega(z_l \sin\theta + x_l \cos\theta)} e^{-i\omega(z_l \sin\theta' + x_l \cos\theta')} \right|$$

Summing over $\mathbf{r}_l, l = 1, ..., m$ results in finite geometric series in the longitudinal and transverse coordinates since they are equally spaced. We obtain

$$\begin{aligned}\frac{np}{m}\left|\sum_{l=1}^{m}\Phi_{jl}\Phi_{li}^{*}\right| &= \frac{1}{m}\left|\frac{e^{i\omega\ell(\cos\theta'-\cos\theta+\cos\tilde{\theta}-\cos\tilde{\theta}')\sqrt{m}/2}-e^{-i\omega(\cos\theta'-\cos\theta+\cos\tilde{\theta}-\cos\tilde{\theta}')\sqrt{m}/2}}{e^{i\omega\ell(\cos\theta'-\cos\theta+\cos\tilde{\theta}-\cos\tilde{\theta}')}-1}\right| \\ &\times\left|\frac{e^{i\omega\ell(\sin\theta'-\sin\theta+\sin\tilde{\theta}-\sin\tilde{\theta})\sqrt{m}/2}-e^{-i\omega(\sin\theta'-\sin\theta+\sin\tilde{\theta}-\sin\tilde{\theta}')\sqrt{m}/2}}{e^{i\omega\ell(\sin\theta'-\sin\theta+\sin\tilde{\theta}-\sin\tilde{\theta}')}-1}\right|. \qquad (86)\end{aligned}$$

Using the identity $|1-e^{i\phi}| = 2|\sin(\phi/2)|$ we then obtain

$$\begin{aligned}\frac{np}{m}\left|\sum_{l=1}^{m}\Phi_{jl}\Phi_{li}^{*}\right| &= \frac{1}{m}\frac{\left|\sin\left[\omega\ell(\cos\theta'-\cos\theta+\cos\tilde{\theta}-\cos\tilde{\theta}')\sqrt{m}/2\right]\right|}{\left|\sin\left[\omega\ell(\cos\theta'-\cos\theta+\cos\tilde{\theta}-\cos\tilde{\theta}')/2\right]\right|} \\ &\times\frac{\left|\sin\left[\omega\ell(\sin\theta'-\sin\theta+\sin\tilde{\theta}-\sin\tilde{\theta}')\sqrt{m}/2\right]\right|}{\left|\sin\left[\omega\ell(\sin\theta'-\sin\theta+\sin\tilde{\theta}-\sin\tilde{\theta}')/2\right]\right|} \qquad (87)\end{aligned}$$

Since θ, θ' are independently and identically distributed according to f^{i}, the sine and cosine of these variables have the density functions

$$g_1^{\mathrm{i}}(t) = \frac{1}{\sqrt{1-t^2}}f^{\mathrm{i}}(\arccos t) \quad \text{and} \quad g_2^{\mathrm{i}}(t) = \frac{1}{\sqrt{1-t^2}}f^{\mathrm{i}}(\arcsin t),$$

respectively. Similarly the sine and cosine of $\tilde{\theta}, \tilde{\theta}'$ have the density functions

$$g_1^{\mathrm{s}}(t) = \frac{1}{\sqrt{1-t^2}}f^{\mathrm{s}}(\arccos t) \quad \text{and} \quad g_2^{\mathrm{s}}(t) = \frac{1}{\sqrt{1-t^2}}f^{\mathrm{s}}(\arcsin t),$$

respectively.

Hence the random variables

$$\begin{aligned}Z_1 &= \omega\ell(\cos\theta'-\cos\theta+\cos\tilde{\theta}-\cos\tilde{\theta}')/2 \quad \in[-2\omega\ell, 2\omega\ell] \\ Z_2 &= \omega\ell(\sin\theta'-\sin\theta+\sin\tilde{\theta}-\sin\tilde{\theta}')/2 \quad \in[-2\omega\ell, 2\omega\ell]\end{aligned}$$

have the density function

$$f_{Z_i} = \frac{1}{\omega\ell}(g_i^{\mathrm{i}} * g_i^{\mathrm{i}} * g_i^{\mathrm{s}} * g_i^{\mathrm{s}})(\frac{2z}{\omega\ell}), \quad i = 1, 2. \qquad (88)$$

Since $g * g * g * g$ is bounded in $[-4, 4]$, we have

$$\|f_{Z_i}\|_\infty \le \frac{c_0}{\omega\ell}, \quad \omega\ell \gg 1, \quad i = 1, 2.$$

for some constant $c_0 > 0$.

Define

$$\zeta = \min_{\theta,\theta',\tilde{\theta},\tilde{\theta}'}\min_{k\in\mathbb{Z}}\{|Z_1-\pi k|, |Z_2-\pi k|\} \qquad (89)$$

and note

$$\sin\zeta > \frac{2\zeta}{\pi}, \quad \zeta\in(0,\pi/2).$$

Hence the probability that $\{\zeta > b\}$ for small $b > 0$ is larger than

$$(1-c_1 b)^{n(n-1)p(p-1)}$$

where the power $n(n-1)p(p-1)$ accounts for the number of different pairs of random variables involved in (89).

By the choice

$$b = \sqrt{\frac{np-1}{m}}$$

we deduce that

$$\mu\left(\mathbf{\Phi}^*\right) < \frac{1}{mb^2} = \frac{1}{np-1}$$

with probability larger than

$$\left(1 - c_1\sqrt{\frac{np-1}{m}}\right)^{n(n-1)p(p-1)}$$

In the SIMO case $p = 1$, (89) becomes

$$\zeta = \min_{\tilde{\theta},\tilde{\theta}'} \min_{k\in\mathbb{Z}} \left\{|Z_1 - \pi k|, |Z_2 - \pi k|\right\}. \tag{90}$$

Hence the probability that $\{\zeta > b\}$ for small $b > 0$ is larger than

$$(1 - c_1 b)^{n(n-1)}$$

With

$$b = \sqrt{\frac{n-1}{m}}$$

it follows that

$$\mu\left(\mathbf{\Phi}^*\right) < \frac{1}{mb^2} = \frac{1}{np-1}$$

with probability larger than

$$\left(1 - c_1\sqrt{\frac{n-1}{m}}\right)^{n(n-1)}.$$

□

5. Proof of Theorem 5: Stability

Next, we give an estimate for the smallest component of the exciting field vector $U = (1 - \omega^2\mathbf{G}\mathcal{V})^{-1}U^{\mathrm{i}}$.

Proposition 7. *If*

$$\omega^2\|\mathbf{G}\mathcal{V}\| < 1/2 \tag{91}$$

then

$$\left\|\frac{1}{\left(\mathbf{I} - \omega^2\mathbf{G}\mathcal{V}\right)^{-1}U^{\mathrm{i}}}\right\|_\infty \leq \frac{1 - \omega^2\|\mathbf{G}\mathcal{V}\|}{1 - 2\omega^2\|\mathbf{G}\mathcal{V}\|} \equiv \frac{1}{b_0}. \tag{92}$$

Here for any vector V, V^{-1} denotes the vector whose entries are the reciprocal of those of V.

Proof. We write

$$\left(\mathbf{I} - \omega^2\mathbf{G}\mathcal{V}\right)^{-1}U^{\mathrm{i}} = U^{\mathrm{i}} \odot (1 \oplus R)$$

with

$$R = (U^{\mathrm{i}})^{-1} \odot \left(\omega^2\mathbf{G}\mathcal{V}U^{\mathrm{i}} + (\omega^2\mathbf{G}\mathcal{V})^2U^{\mathrm{i}} + ...\right)$$

which converges under (91). Here $\odot$ and $\oplus$ denote the entrywise (Hadamard) product and sum, respectively, of two vectors. Hence

$$\left\|\frac{1}{\left(\mathbf{I} - \omega^2\mathbf{G}\mathcal{V}\right)^{-1}U^{\mathrm{i}}}\right\|_\infty \leq \left\|\frac{1}{U^{\mathrm{i}} \odot (1 \oplus R)}\right\|_\infty \leq \frac{1}{1 - \|R\|_\infty}. \tag{93}$$

We also have

$$\|R\|_\infty \leq \left(\omega^2\|\mathbf{G}\mathcal{V}\| + \omega^4\|\mathbf{G}\mathcal{V}\|^2 + ...\right) = \frac{\omega^2\|\mathbf{G}\mathcal{V}\|}{1-\omega^2\|\mathbf{G}\mathcal{V}\|}. \tag{94}$$

Substituting (94) into (93) we obtain the claimed bound (92). □

From the Foldy-Lax equation (36) and (92) we have the following lower bound on the exciting field vector U

$$\left\|U^{-1}\right\|_\infty \leq 1/b_0 \tag{95}$$

and hence $b_0 \leq |u(\mathbf{r}_{i_j})|, \forall j$.

Corollary 3. *Suppose* $\mu(\mathbf{\Phi})s \leq 1/3$ *and*

$$b_0 > \left(3+\sqrt{3/2}\right)\varepsilon\|\mathcal{V}^{-1}\|. \tag{96}$$

Then $\mathrm{supp}(\hat{X}) = \mathrm{supp}(X)$.

Proof. This follows immediately from the fact

$$\min_j |X_j| = \min_j |\nu_{i_j} u(\mathbf{r}_{i_j})| \geq \frac{b_0}{\|\mathcal{V}^{-1}\|} > (3+\sqrt{3/2})\varepsilon$$

and Proposition 4. □

Proposition 8. *The vector* $U^{\mathrm{i}} + \omega^2\mathbf{G}\hat{X}$ *contains no zero entry if* $\omega^2\|\mathbf{G}\hat{X}\|_\infty < 1$. *In particular, this is true for the minimizer* $\hat{X}$ *of Proposition 4 under the additional assumption*

$$b_0 > \omega^2(3+\sqrt{3/2})\varepsilon\|\mathbf{G}\|. \tag{97}$$

In this case, $\mathrm{supp}(\hat{\mathcal{V}}) = \mathrm{supp}(\hat{X})$.

Proof. The following calculation is straightforward

$$\|\mathbf{G}\hat{X} - \mathbf{G}X\|_\infty \leq \|\mathbf{G}\|\|\hat{X} - X\|_\infty \leq (3+\sqrt{3/2})\varepsilon\|\mathbf{G}\|. \tag{98}$$

Moreover, since

$$\mathbf{G}X = \mathbf{G}\mathcal{V}(\mathbf{I} - \omega^2\mathbf{G}\mathcal{V})^{-1}U^{\mathrm{i}}$$

we have the estimate

$$\|\mathbf{G}X\|_\infty \leq \frac{\|\mathbf{G}\mathcal{V}\|}{1-\omega^2\|\mathbf{G}\mathcal{V}\|}. \tag{99}$$

Hence

$$\begin{aligned} \omega^2\|\mathbf{G}\hat{X}\|_\infty &\leq \omega^2\|\mathbf{G}X\|_\infty + \omega^2\|\mathbf{G}\hat{X} - \mathbf{G}X\|_\infty \\ &\leq \frac{\omega^2\|\mathbf{G}\mathcal{V}\|}{1-\omega^2\|\mathbf{G}\mathcal{V}\|} + \omega^2(3+\sqrt{3/2})\varepsilon\|\mathbf{G}\| \\ &= 1 - b_0 + \omega^2(3+\sqrt{3/2})\varepsilon\|\mathbf{G}\| < 1 \end{aligned} \tag{100}$$

under the additional condition (97). □

The proof of Theorem 5 can now be completed as follows.

Proof. First of all, (52) is equivalent to (97) and by Proposition 8 the formula (50) is well-defined.

Subtracting (41) from (50) we can estimate as follows:

$$\begin{aligned}\|\mathcal{V}-\hat{\mathcal{V}}\| &= \left\|\frac{U^{\mathrm{i}}\odot(X-\hat{X})+\omega^2(X-\hat{X})\odot\mathbf{G}X-\omega^2X\odot\mathbf{G}(X-\hat{X})}{(U^{\mathrm{i}}+\omega^2\mathbf{G}\hat{X})(U^{\mathrm{i}}+\omega^2\mathbf{G}X)}\right\| \\ &\leq \frac{\left(1+\omega^2\|\mathbf{G}X\|_\infty\right)\|X-\hat{X}\|_\infty+\omega^2\|X\|_\infty\|\mathbf{G}X-\mathbf{G}\hat{X}\|_\infty}{1-\omega^2\|\mathbf{G}\hat{X}\|_\infty}\times\|U^{-1}\|_\infty\end{aligned}$$

where we have used the identity

$$U=\omega^2\mathbf{G}X+U^{\mathrm{i}}. \tag{101}$$

By (91) and (99) we find that

$$\omega^2\|\mathbf{G}X\|_\infty < 1 \tag{102}$$

And, since $X=(\nu_j u(\mathbf{r}_j))$,

$$\|X\|_\infty\leq\|\mathcal{V}\|\|U\|_\infty.$$

This, (95), (98) and Proposition 4 lead to the bound

$$\|\mathcal{V}-\hat{\mathcal{V}}\|\leq\frac{(2+\omega^2\|\mathbf{G}\|\|\mathcal{V}\|\|U\|_\infty)(3+\sqrt{3/2})\varepsilon}{b_0(b_0-\omega^2(3+\sqrt{3/2})\varepsilon\|\mathbf{G}\|)}. \tag{103}$$

In view of (101) and (99) we have the following bound

$$\|U\|_\infty \leq 1+\omega^2\|\mathbf{G}X\|_\infty \leq\frac{1}{1-\omega^2\|\mathbf{G}\mathcal{V}\|}<2. \tag{104}$$

The claimed result (53) now follows from (103) and (104).

Since (54) is equivalent with (96) it follows from Corollary 3, Propositions 8 and 3 that $\mathrm{supp}(\hat{\mathcal{V}})=\mathrm{supp}(\mathcal{V})$. □

6. Proof of Theorem 6

Let $\mathbf{d}=(\alpha,\beta,\gamma)$ be parameterized by the angles θ,ϕ as

$$\alpha=\cos\theta\cos\phi,\quad \beta=\cos\theta\sin\phi,\quad \gamma=\sin\theta. \tag{105}$$

The pairwise coherence has the form

$$\frac{1}{pn}\sum_{k=1}^{p}e^{i\omega(\alpha_k,\beta_k,\gamma_k)\cdot(\mathbf{r}-\mathbf{r}')}\sum_{j=1}^{n}e^{i\omega(\tilde{\alpha}_j,\tilde{\beta}_j,\tilde{\gamma}_j)\cdot(\mathbf{r}-\mathbf{r}')} \tag{106}$$

where $(\alpha_k,\beta_k,\gamma_k),k=1,...,p$ and $(\tilde{\alpha}_j,\tilde{\beta}_j,\tilde{\gamma}_j),j=1,...,n$ are independently and identically distributed in the *unit* sphere according to $f^{\mathrm{i}}(\theta,\phi)$ and $f^{\mathrm{s}}(\theta,\phi)$, respectively.

The main difference between two and three dimensions is in evaluating the expectation of $p^{-1}\sum_{k=1}^{p}e^{i\omega(\alpha_k,\beta_k,\gamma_k)\cdot(\mathbf{r}-\mathbf{r}')}$ and $n^{-1}\sum_{j=1}^{n}e^{i\omega(\tilde{\alpha}_j,\tilde{\beta}_j,\tilde{\gamma}_j)\cdot(\mathbf{r}-\mathbf{r}')}$ which amounts to calculating the integrals

$$\int_{-\pi/2}^{\pi/2}d\theta f_1^{\mathrm{i}}(\theta+\theta_0)\cos\theta\exp\left[i\omega|\mathbf{r}-\mathbf{r}'|\sin\theta\right] \tag{107}$$

$$\int_{-\pi/2}^{\pi/2}d\theta f_1^{\mathrm{s}}(\theta+\theta_0)\cos\theta\exp\left[i\omega|\mathbf{r}-\mathbf{r}'|\sin\theta\right] \tag{108}$$

for some θ_0 depending on $\mathbf{r}-\mathbf{r}'$ where $f_1^{\rm i}$ and $f_1^{\rm s}$ are the marginal density functions

$$\begin{aligned} f_1^{\rm i}(\theta) &= \int_{-\pi}^{\pi} d\phi f^{\rm i}(\theta,\phi) \\ f_1^{\rm s}(\theta) &= \int_{-\pi}^{\pi} d\phi f^{\rm s}(\theta,\phi) \end{aligned}$$

If $f_1^{\rm i}=f_1^{\rm s}=1/\pi$, the integrals (107) and (108) become

$$\frac{2\sin\left(\omega|\mathbf{r}-\mathbf{r}'|\right)}{\omega|\mathbf{r}-\mathbf{r}'|}=\mathcal{O}(\frac{1}{\omega\ell}),\quad \omega\ell\gg 1.$$

For the general case, integrating by parts with (107) and (108) produces

$$\frac{i}{\omega|\mathbf{r}-\mathbf{r}'|}\left[f_1^{\rm i}(\theta+\theta_0)e^{i\omega|\mathbf{r}-\mathbf{r}'|\sin\theta}\Big|_{-\pi/2}^{\pi/2}-\int_{-\pi/2}^{\pi/2}e^{i\omega|\mathbf{r}-\mathbf{r}'|\sin\theta}\frac{d}{d\theta}f_1^{\rm i}(\theta+\theta_0)d\theta\right] \tag{109}$$

$$\frac{i}{\omega|\mathbf{r}-\mathbf{r}'|}\left[f_1^{\rm s}(\theta+\theta_0)e^{i\omega|\mathbf{r}-\mathbf{r}'|\sin\theta}\Big|_{-\pi/2}^{\pi/2}-\int_{-\pi/2}^{\pi/2}e^{i\omega|\mathbf{r}-\mathbf{r}'|\sin\theta}\frac{d}{d\theta}f_1^{\rm s}(\theta+\theta_0)d\theta\right] \tag{110}$$

from which we obtain the bound

$$\left|\int_{-\pi/2}^{\pi/2}d\theta f_1^{\rm i}(\theta+\theta_0)\cos\theta\exp\left[i\omega|\mathbf{r}-\mathbf{r}'|\sin\theta\right]\right|\le\frac{c}{1+\omega\ell}\|f^{\rm i}\|_{1,\infty} \tag{111}$$

$$\left|\int_{-\pi/2}^{\pi/2}d\theta f_1^{\rm s}(\theta+\theta_0)\cos\theta\exp\left[i\omega|\mathbf{r}-\mathbf{r}'|\sin\theta\right]\right|\le\frac{c}{1+\omega\ell}\|f^{\rm s}\|_{1,\infty}. \tag{112}$$

7. Proof of Theorem 7

7.1. **Two dimensional case.** The pairwise coherence is a ratio of the numerator

$$\frac{1}{n}\left|\sum_{j=1}^{n}G^*(\mathbf{a}_j-\mathbf{r})G(\mathbf{a}_j-\mathbf{r}')\right| \tag{113}$$

and the denominator

$$\frac{1}{n}\left(\sum_{j=1}^{n}|G(\mathbf{a}_j-\mathbf{r})|^2\right)^{1/2}\cdot\left(\sum_{j=1}^{n}|G(\mathbf{a}_j-\mathbf{r}')|^2\right)^{1/2} \tag{114}$$

with $\mathbf{r}=(x,z),\mathbf{r}'=(x',z')$ being two distinct elements of $\{\mathbf{r}_l,l=1,...,m\}$. Note that $G^*(\mathbf{a}_j-\mathbf{r})G(\mathbf{a}_j-\mathbf{r}')$ are i.i.d. random variables since $\mathbf{a}_j$ are.

To analyze the summation in (113) we follow the argument of the proof of Theorem 1. Define the random variables $P_j,Q_j,j=1,...,n$ to be the real and imaginary parts, respectively, of $G^*(\mathbf{a}_j-\mathbf{r})G(\mathbf{a}_j-\mathbf{r}')$. We apply the Hoeffding inequality to both $S_n=\sum_{j=1}^n P_j$ and $T_n=\sum_{j=1}^n Q_j$.

Note that the ranges $r_0=b_j-a_j$ of P_j and Q_j depends on the minimum distance $\Delta_{\min}$ between $\{z=0\}$ and the square lattice (Figure 4). Indeed for small distance $\Delta_{\min}\ll 1$, $r_0=O(-\log\Delta_{\min})$. We have

$$\begin{aligned}&\mathbb{P}\left[\max_{i\neq j}\frac{1}{n}\left|\sum_{j=1}^{n}\left[G^*(\mathbf{a}_j-\mathbf{r})G(\mathbf{a}_j-\mathbf{r}')-\mathbb{E}\left(G^*(\mathbf{a}_j-\mathbf{r})G(\mathbf{a}_j-\mathbf{r}')\right)\right]\right|<\sqrt{2}K/\sqrt{n}\right] \\ &>(1-\delta)^2\end{aligned} \tag{115}$$

if (66) holds.

Using (61) we have the following calculation for the expectation:

$$\begin{aligned}
&\mathbb{E}\left\{G^*(\mathbf{a}_j-\mathbf{r})G(\mathbf{a}_j-\mathbf{r}')\right\}\\
&= \frac{1}{16\pi^2}\int \frac{d\alpha}{\gamma^*}\frac{d\alpha'}{\gamma'}\mathbb{E}\left\{e^{-i\omega(z\gamma^*+(\xi_j-x)\alpha)}e^{i\omega(z'\gamma'+(\xi_j-x')\alpha')}\right\}\\
&= \frac{1}{16\pi^2}\int \frac{d\alpha}{\gamma^*}\frac{d\alpha'}{\gamma'}e^{i\omega(-z\gamma^*+z'\gamma')}e^{i\omega(\alpha x-\alpha' x')}\frac{2\sin\left((\alpha'-\alpha)\omega L/2\right)}{\omega L(\alpha'-\alpha)}. \qquad (116)
\end{aligned}$$

We divide the integration (116) into three parts: $I_i, i=1,2,3$, the integrals over, respectively,

$$\begin{aligned}
R_1 &= \{|\alpha|>\sqrt{2}\}\cup\{|\alpha'|>\sqrt{2}\},\\
R_2 &= R_1^c\cap\{|\alpha-\alpha'|<H/(\omega L)\},\\
R_3 &= R_1^c\cap\{|\alpha-\alpha'|>H/(\omega L)\}
\end{aligned}$$

where $H\ll\omega L$ will be determined later.

To estimate I_1, note that

$$\lim_{\varepsilon\to 0}\frac{2\sin\left((\alpha'-\alpha)/\varepsilon\right)}{\alpha'-\alpha}=\delta(\alpha'-\alpha)\quad\text{in the sense of distribution.}$$

Consequently $\omega L\cdot|I_1|$ tends to

$$\frac{1}{16\pi^2}\left|\int_{|\alpha|>\sqrt{2}}\frac{d\alpha}{|\gamma|^2}e^{-\omega|z+z'||\gamma|}e^{i\omega\alpha(x-x')}\right| \;\le\; \frac{e^{-2\omega\Delta_{\min}}}{16\pi^2}\left|\int_{|\alpha|>\sqrt{2}}\frac{d\alpha}{|\gamma|^2}\right|,\quad \omega L\to\infty,$$

and hence is bounded uniformly in $\omega\Delta_{\min}>0$.

For I_2 and I_3 we have the rough estimates

$$\begin{aligned}
|I_2| &\le \frac{1}{16\pi^2}\int_{R_2}\frac{d\alpha d\alpha'}{|\gamma\gamma'|}=\mathcal{O}\left(\frac{H}{\omega L}\right)\\
|I_3| &\le \frac{1}{16\pi^2}\int_{R_3}\frac{d\alpha d\alpha'}{|\gamma\gamma'|}\frac{1}{H}=\mathcal{O}\left(\frac{1}{H}\right)
\end{aligned}$$

where the singularities are inverse-square-root and hence integrable. By choosing $H=\sqrt{\omega L}$ we obtain

$$\left|\mathbb{E}\left\{G^*(\mathbf{a}_j-\mathbf{r})G(\mathbf{a}_j-\mathbf{r}')\right\}\right|\le\frac{c_1}{\sqrt{\omega L}},\quad \omega L\gg 1 \qquad (117)$$

for some constant $c_1>0$.

A simple lower bound for the expression (114) is given by

$$\min_{\mathbf{a},\mathbf{r}}|G(\mathbf{a}-\mathbf{r})|^2 \qquad (118)$$

where $\mathbf{a}$ runs through the entire square aperture of length L and $\mathbf{r}$ runs through the entire square domain of length $\ell\sqrt{m}$. Since $|G|$ is a decreasing function of the absolute value of its argument, (118) is achieved by the pair of points furthest away from each other. In the assumed imaging geometry, Figure 4, the largest distance $\Delta_{\max}$ between any pair of points is given by (62). Combining (115, (117) and (118) we obtain that (67) as claimed.

7.2. **Three dimensional case.** We now need to estimate (113) and (114) with $\mathbf{r} = (x, y, z), \mathbf{r}' = (x', y', z')$ being two distinct elements of $\{\mathbf{r}_l, l = 1, ..., m\}$. We proceed as before.

Define the random variables $P_j, Q_j, j = 1, ..., n$ to be the real and imaginary parts, respectively, of $G^*(\mathbf{a}_j - \mathbf{r})G(\mathbf{a}_j - \mathbf{r}')$. In three dimensions, the ranges r_0 of P_j and Q_j are $\mathcal{O}(\Delta_{\min}^{-1})$.

Using (64) we have the following calculation:

$$\begin{aligned}
&\frac{1}{\omega^2}\mathbb{E}\left\{G^*(\mathbf{a}_j - \mathbf{r})G(\mathbf{a}_j - \mathbf{r}')\right\} \\
&= \frac{1}{64\pi^4}\int \frac{d\alpha d\beta}{\gamma^*}\frac{d\alpha' d\beta'}{\gamma'}\mathbb{E}\left\{e^{-i\omega(z\gamma^* + (\xi_j - x)\alpha + (\eta_j - y)\beta)}e^{i\omega(z'\gamma' + (\xi_j - x')\alpha' + (\eta_j - y')\beta')}\right\} \\
&= \frac{1}{64\pi^4}\int \frac{d\alpha d\beta}{\gamma^*}\frac{d\alpha' d\beta'}{\gamma'}e^{i\omega(-z\gamma^* + z'\gamma')}e^{i\omega(\alpha x - \alpha' x')}e^{i\omega(\beta y - \beta' y')} \\
&\quad \cdot\frac{2\sin\left((\alpha' - \alpha)\omega L/2\right)}{\omega L(\alpha' - \alpha)} \cdot \frac{2\sin\left((\beta' - \beta)\omega L/2\right)}{\omega L(\beta' - \beta)}.
\end{aligned}$$

We divide the integration into several parts as follows. Denote

$$\begin{aligned}
A_1 &= \{|\alpha| > 1\} \cup \{|\alpha'| > 1\}, \\
A_2 &= \{|\alpha - \alpha'| > H/(\omega L)\}, \\
B_1 &= \{|\beta| > 1\} \cup \{|\beta'| > 1\}, \\
B_2 &= \{|\beta - \beta'| > H/(\omega L)\}.
\end{aligned}$$

Let $I_i, i = 1, 2, 3, 5, 6, 7$, be the integrals over, respectively, $R_1 = A_1 \cap B_1, R_2 = A_1^c \cap B_1, R_3 = A_1 \cap B_1^c, R_4 = A_1^c \cap B_1^c$.

I_1 can be estimated straightforwardly by

$$I_1 \leq \frac{c}{64\pi^4\omega^2 L^2}\int_{R_1} e^{-\omega\gamma(z+z')}\frac{d\alpha d\beta}{|\gamma|^2}$$

for a constant c and is bounded uniformly in $\omega > 1$.

I_2 can be further decomposed into two parts parts $I_{2i}, i = 1, 2$ corresponding, respectively, to integration over $R_{21} = A_1^c \cap B_1 \cap A_2, R_{22} = A_1^c \cap B_1 \cap A_2^c$ and estimated by

$$I_2 = I_{21} + I_{22} \leq \frac{c}{64\pi^4}\int \frac{d\alpha d\beta d\alpha' d\beta'}{|\gamma\gamma'|}\left(\frac{1}{H} + \frac{H}{\omega L}\right)\cdot\frac{1}{\omega L}$$

for a constant c.

I_3 can be further decomposed into two parts $I_{3i}, i = 1, 2$, corresponding, respectively, to integration over $R_{31} = A_1 \cap B_1^c \cap B_2^c, R_{32} = A_1 \cap B_1^c \cap B_2$ and estimated by

$$I_3 = I_{31} + I_{32} \leq \frac{c}{64\pi^4}\int \frac{d\alpha d\beta d\alpha' d\beta'}{|\gamma\gamma'|}\left(\frac{1}{H} + \frac{H}{\omega L}\right)\cdot\frac{1}{\omega L}$$

for a constant c.

I_4 can be decomposed into four parts $I_{4i}, i = 1, 2, 3, 4$ corresponding, respectively, to integration over

$$\begin{aligned}
R_{41} &= A_1^c \cap A_2 \cap B_1^c \cap B_2, \\
R_{42} &= A_1^c \cap A_2 \cap B_1^c \cap B_2^c, \\
R_{43} &= A_1^c \cap A_2^c \cap B_1^c \cap B_2, \\
R_{44} &= A_1^c \cap A_2^c \cap B_1^c \cap B_2^c,
\end{aligned}$$

and estimated by

$$I_4 = \sum_{i=1}^{4} I_{4i} \leq \frac{c}{64\pi^4} \int \frac{d\alpha d\beta d\alpha' d\beta'}{|\gamma\gamma'|} \left(\frac{1}{H} \cdot \frac{1}{H} + \frac{1}{H} \cdot \frac{H}{\omega L} + \frac{H}{\omega L} \cdot \frac{1}{H} + \frac{H}{\omega L} \cdot \frac{H}{\omega L} \right)$$

for some constant c.

Setting $H = (\omega L)^{1/2}$ we obtain

$$\frac{1}{\omega^2} \mathbb{E} \left\{ G^*(\mathbf{a}_j - \mathbf{r}) G(\mathbf{a}_j - \mathbf{r}') \right\} \leq \frac{c_2}{\omega L}, \quad \omega L \gg 1$$

for some constant $c_2 > 0$.

Using (118) for the lower bound of (114) we conclude (68) in Theorem 7.

8. Conclusion

We have analyzed the SIMO/MISO and MIMO inverse scattering problems by compressed sensing theory to shed new light on this problem with distinguished history [13, 30, 35, 44]. We have obtained several main results: Theorem 3 concerns the recoverability by L^1 minimization with the MIMO measurement under the Born approximation, Theorem 4 addresses the recoverability by L^1 minimization with the SIMO/MISO measurement including multiple scattering and Theorem 5 asserts stability to measurement or model errors for weak or widely separated scatterers under a stronger sparsity constraint. We have also analyzed the diffraction tomography with few views and limited angles and proved the coherence bound (Theorem 7) analogous to Theorem 3.

A main limitation to our approach is the assumption of finite (albeit high) dimensional targets. Also, the reconstruction succeeds only probabilistically. These limitations are intrinsic to the current formulation of the compressed sensing theory which is still evolving and in this regard the present paper is only a first step in the new direction.

On the other hand, the compressed sensing approach is constructive and treats the uniqueness and the reconstruction in a unified way. Indeed, the main advantage of this approach is an explicit and efficient method (i.e. the Basis Pursuit with the SIMO/MIMO or MIMO sensing matrix) for reconstructing the scatterers from the scattering amplitude. Moverover, the aperture can be rather arbitrary and the dimension of measurement can be as low as comparable to the target sparsity (up to a $\log(m)$-factor).

It may be worthwhile to compare our imaging method with the MUSIC algorithm which employs multiple sensors to collect the $n \times n$ multistatic response data matrix where n is the number of transmitters/receivers [12, 46]. When the measurement is carried out in the far field, the (l, j)-entry of the response matrix is the measured scattering amplitude for the sampling direction l and the incident direction j. It is not known if MUSIC can recover the target support exactly for nonlinear inverse scattering. Only the case for the Born approximation has been shown capable of exact recovery of the target *support* in the absence of noise [27] (see the corrected argument in Theorem 4.1, [28]). And the estimate for the required dimension of the measurement for the exact recovery is hardly optimal. This result should be compared to Theorem 3 with $p = n$ and $\theta_j = -\tilde{\theta}_j, j = 1, ..., n$, in particular the sparsity constraint (29) for compressed sensing versus the necessary condition $n > s$ for MUSIC. This represents a significant reduction in the number of sensors when the sparsity of the target vector is large.

In a separate paper [20] we propose novel multi-shot single-input-single-output (SISO) compressive imaging methods and demonstrate their superior performances including the capability of imaging *extended* targets. We also present in [20] numerical comparative study of the respective performances of the SIMO/MIMO and multi-shot SISO schemes.

References

[1] M. Born and E. Wolf, *Principles of Optics*, 7-th edition, Cambridge University Press, 1999.

[2] S. Boyd and L. Vandenberghe, *Convex Optimization.* Cambridge University Press, Cambridge, 2004.

[3] A.M. Bruckstein, D.L. Donoho and M. Elad, "From sparse solutions of systems of equations to sparse modeling of signals," *SIAM Rev.* **51** (2009), 34-81.

[4] E. J. Candès, "The restricted isometry property and its implications for compressed sensing," *Compte Rendus de l'Academie des Sciences, Paris, Serie I.* **346** (2008) 589-592.

[5] E. J. Candès, J. Romberg and T. Tao, "Robust undertainty principles: Exact signal reconstruction from highly incomplete frequency information," *IEEE Trans. Inform. Theory* **52** (2006), 489-509.

[6] E.J. Candès, J. Romberg and T. Tao, "Stable signal recovery from incomplete and inaccurate measurements," *Commun. Pure Appl. Math.* **59** (2006), 120723.

[7] E.J. Candès and Y. Plan, "Near-ideal model selection by ℓ_1 minimization," preprint, 2008.

[8] E. J. Candès and T. Tao, " Decoding by linear programming," *IEEE Trans. Inform. Theory* **51** (2005), 42034215.

[9] E. J. Candès and T. Tao, " Near-optimal signal recovery from random projections: universal encoding strategies?," *IEEE Trans. Inform. Theory* **52** (2006), 54-6-5425.

[10] L. Carin, D. Liu and B. Guo, "In Situ Compressive Sensing for Multi-Static Scattering: Imaging and the Restricted Isometry Property", preprint, 2008.

[11] S.S. Chen, D.L. Donoho and M.A. Saunders, "Atomic decomposition by basis pursuit," *SIAM Rev.* **43** (2001), 129-159.

[12] M. Cheney, "The linear sampling method and MUSIC algorithm," *Inverse Problems* **17** (2001), 591-596.

[13] D. Colton, J. Coyle and P. Monk, "Recent developments in inverse acoustic scattering theory," *SIAM Rev.* **42** (2000), 369-414.

[14] D. Colton and R. Kress, *Inverse Acoustic and Electromagnetic Scattering Theory.* 2nd edition, Springer, 1998.

[15] W. Dai and O. Milenkovic, "Subspace pursuit for compressive sensing: closing the gap between performance and complexity," arXiv:0803.0811.

[16] I. Daubechies, *Ten Lectures on Wavelets.* SIAM, Philadelphia, 1992.

[17] D.L. Donoho and M. Elad, "Optimally sparse representation in general (nonorthogonal) dictionaries via ℓ^1 minimization," *Proc. Nat. Acad. Sci.* **100** (2003) 2197-2202.

[18] D.L. Donoho and X. Huo, "Uncertainty principle and ideal atomic decomposition, " *IEEE Trans. Inform. Theory* **47** (2001), 2845-2862.

[19] B. Efron, T. Hastie, I. Johnstone and R. Tibshirani, "Least angle regression". *Ann. Statist.* **32** (2004), 407451.

[20] A. Fannjiang, "Compressive inverse scattering II. SISO measurements with Born scatterers," to appear.

[21] A. Fannjiang, "Compressive imaging of subwavelength structures," *SIAM J. Imag. Sci.* **2** (2009), 1277-1291.

[22] A. Fannjiang, P. Yan and Thomas Strohmer, "Compressed remote sensing of sparse objects," `arXiv:0904.3994`

[23] R. Gribonval and M. Nielsen, "Sparse representation in unions of bases," *IEEE Trans. Inform. Theory* **49** (2003), 3320-3325.

[24] G.M. Henkin and R.G. Novikov, "A multidimensional inverse problem in quantum and acoustic scattering, "*Inverse Problems* **4** (1988) 103-121.

[25] F. J. Herrmann, "Compressive imaging by wavefield inversion with group sparsity," preprint, 2009.

[26] W. Hoeffding, "Probability inequalities for sums of bounded random variables", *J. Amer. Stat. Assoc.* **58** (1963) 1330.

[27] A. Kirsch, "The MUSIC-algorithm and the factorization method in inverse scattering theory for inhomogeneous media," *Inverse Problems* **18** (2002) 1025-1040.

[28] A. Kirsch and N. Grinsberg, *The Factorization Method for Inverse Problems,* Oxford University Press, Oxford, 2008.

[29] R. Kohn and M. Vogelius, "Determining conductivity by boundary measurements," *Comm. Pure Appl. Math.* **37** (1984), 113-123.

[30] P. D. Lax and R. S. Phillips, *Scattering Theorey,* Revised Edition. Academic Press, San Diego, 1989.

[31] A. Majda, "High frequency asymptotics for the scattering matrix and inverse problem of acoustical scattering," *Comm. Pure Appl. Math.***29** (1976) 261-291.

[32] E.A. Marengo, "Inverse scattering by compressive sensing and signal subspace methods", *IEEE Workshop on Computational Advances in Multi-Sensor Adaptive Processing (CAMSAP)*, St. Thomas, U.S. Virgin Islands, Dec. 12-14, 2007.

[33] E.A. Marengo and F.K. Gruber, Subspace-based localization and inverse scattering of multiply scattering point targets, *EURASIP J. Advances in Signal Processing* **2007**, Article ID 17342, 16 pages, 2007.

[34] E.A. Marengo, R.D. Hernandez, Y.R. Citron, F.K. Gruber, M. Zambrano, and H. Lev-Ari, "Compressive sensing for inverse scattering", *XXIX URSI General Assembly*, Chicago, Illinois, Aug. 7-16, 2008.

[35] R.B. Melrose, *Geometric Scattering Theory*, Cambridge University Press, Cambridge, 1995.
[36] M. I. Mishchenko, L. D. Travis, and A. A. Lacis, *Multiple Scattering of Light by Particles: Radiative Transfer and Coherent Backscattering* (Cambridge U. Press, Cambridge, UK, 2006).
[37] A. Nachman, "Reconstruction from boundary measurements," *Ann. Math.* **128** (1988), 531-576.
[38] A. Nachman, "Global uniqueness for a two-dimensional inverse boundary value problem," *Ann. Math.* **143** (1996), 71-96.
[39] D. Needell, J. A. Tropp, and R. Vershynin, "Greedy signal recovery review," *Proc. 42nd Asilomar Conference on Signals, Systems, and Computers*, Pacific Grove, CA, Oct. 2008.
[40] R.G. Novikov, "The inverse scattering problem on a fixed energy level for two-dimensional Schrödinger operator," *J. Funct. Anal.* **103** (1992), 409-463.
[41] R.G. Novikov, "The inverse scattering problem at fixed energy for the three-dimensional Schrdinger equationwith an exponentially decreasing potential." *Commun. Math. Phys.* **161** (1994), 56995.
[42] J. Provost and F. Lesage, "The application of compressed sensing for photo-acoustic tomography," *IEEE Trans. Med. Imag.* **28** (2009), 585-594.
[43] A.G. Ramm, "Recovery of the potential from fixed energy scattering data," *Inverse Problems* **4** (1988), 877-886.
[44] M. Reed and B. Simon, *Methods of Modern Mathematical Physics III. Scattering Theory.* Academic Press, San Diego, 1979.
[45] J. Sylvester and G. Uhlmann, " A global uniqueness theorem for an inverse problem boundary value problem," *Ann. Math.* **125** (1987) 153-169.
[46] C.W. Therrien, *Discrete Random Signals and Statistical Signal Processing*, Englewood Cliffs, NJ: Prentice- Hall, 1992.
[47] R. Tibshirani, "Regression shrinkage and selection via the lasso," J. Roy. Statist. Soc. Ser. B **58** (1996), 267-288.
[48] J.A. Tropp, "Greed is good: algorithmic results for sparse approximation," *IEEE Trans. Inform. Theory* **50** (2004), 2231-2242.
[49] J.A. Tropp, " Just relax: convex programming methods for identifying sparse signals in noise," *IEEE Trans. Inform. Theory* **52** (2006), 1030-1051. "Corrigendum" *IEEE Trans. Inform. Theory* (2008).
[50] J.A. Tropp, "On the conditioning of random subdictionaries," preprint, 2007.
[51] L. Tsang, J. A. Kong, K.-H. Ding, and C. O. Ao, *Scattering of Electromagnetic Waves: Numerical Simulations*, John Wiley & Sons, New York, NY, USA, 2001.
[52] H.C. van de Hulst, *Light Scattering by Small Particles.* Dover Publications, New York, 1981.
[53] J.C. Ye and S. Y. Lee, "Non-iterative exact inverse scattering using simultanous orthogonal matching pursuit (S-OMP)." *IEEE Int. Conf. on Acoustics, Speech, and Signal Processing (ICASSP)*, Las Vegas, Nevada, April 2008.

Appendix A. Input-output reciprocity

More generally, consider the Helmholtz equation with a source

$$\Delta u(\mathbf{r}) + \omega^2(1+\nu(\mathbf{r}))u(\mathbf{r}) = -f(\mathbf{r})$$

which can be solved by using the Green function $\mathcal{G}$ as

$$u(\mathbf{r}) = \int \mathcal{G}(\mathbf{r},\mathbf{r}')f(\mathbf{r}')d\mathbf{r}'.$$

By slight abuse of notation, we shall write the solution as

$$u = \mathcal{G}f$$

where $\mathcal{G}$ stands also for the corresponding propagator.

Because the incident wave is governed by

$$\Delta u^{\mathrm{i}}(\mathbf{r}) + \omega^2 u^{\mathrm{i}}(\mathbf{r}) = -f(\mathbf{r})$$

we can write

$$\begin{aligned} u(\mathbf{r}) &= -\mathcal{G}\left[\Delta u^{\mathrm{i}} + \omega^2 u^{\mathrm{i}}\right](\mathbf{r}) \\ &= \mathcal{G}\left[-(\Delta + \omega^2(1+\nu))u^{\mathrm{i}} + \omega^2\nu u^{\mathrm{i}}\right](\mathbf{r}) \\ &= u^{\mathrm{i}}(\mathbf{r}) + \omega^2\mathcal{G}\left[\nu u^{\mathrm{i}}\right](\mathbf{r}). \end{aligned}$$

Hence the scattered wave $u^{\rm s} = u - u^{\rm i}$ can be expressed as

$$u^{\rm s}(\mathbf{r}) = \omega^2 \int \mathcal{G}(\mathbf{r},\mathbf{r}')\nu(\mathbf{r}')u^{\rm i}(\mathbf{r}')d\mathbf{r}' \tag{119}$$

which is the reciprocal representation to (4).

For point scatterers, (119) becomes

$$u^{\rm s}(\mathbf{r}) = \omega^2 \sum_{j=1}^{m} \nu_j \mathcal{G}(\mathbf{r},\mathbf{r}_j)u^{\rm i}(\mathbf{r}_j), \quad \mathbf{r} \neq \mathbf{r}_k,\ k = 1, ..., s. \tag{120}$$

Substituting the Foldy-Lax equation

$$\mathcal{G}(\mathbf{r},\mathbf{r}_j) = G(\mathbf{r},\mathbf{r}_j) + \omega^2 \sum_{k\neq j} \nu_k \mathcal{G}(\mathbf{r}_j,\mathbf{r}_k)G(\mathbf{r},\mathbf{r}_k), \quad \mathbf{r} \neq \mathbf{r}_j,\ j = 1, ..., s \tag{121}$$

in (120) we obtain

$$u^{\rm s}(\mathbf{r}) = \omega^2 \sum_{j=1}^{m} \nu_j u^{\rm i}(\mathbf{r}_j)G(\mathbf{r},\mathbf{r}_j) + \omega^4 \sum_{j=1}^{m}\sum_{k\neq j} \nu_j\nu_k \mathcal{G}(\mathbf{r}_j,\mathbf{r}_k)u^{\rm i}(\mathbf{r}_j)G(\mathbf{r},\mathbf{r}_j)$$

which can be rewritten as

$$\begin{aligned} u^{\rm s}(\mathbf{r}) &= \sum_{j=1}^{m}\sum_{k=1}^{m} \delta_{j,k}\omega^2\nu_k u^{\rm i}(\mathbf{r}_k)G(\mathbf{r},\mathbf{r}_j) + \omega^4 \sum_{j=1}^{m}\sum_{k\neq j} \nu_j\nu_k \mathcal{G}(\mathbf{r}_j,\mathbf{r}_k)u^{\rm i}(\mathbf{r}_k)G(\mathbf{r},\mathbf{r}_j) \\ &= \sum_{j=1}^{m}\sum_{k=1}^{m} \left[\delta_{j,k}\omega^2\nu_k + (1-\delta_{j,k})\omega^4\nu_j\nu_k\mathcal{G}(\mathbf{r}_j,\mathbf{r}_k)\right] u^{\rm i}(\mathbf{r}_k)G(\mathbf{r},\mathbf{r}_j) \end{aligned} \tag{122}$$

(see [33, 32] for a similar, but slightly erroneous, expression).

To obtain the alternative expression for the scattering amplitude, let $\mathbf{r} \to \infty$ in (122) and extract the plane wave spectrum by (61) for $d = 2$ or (64) for $d = 3$. The scattering amplitude in the direction $\hat{\mathbf{r}}$ is given by

$$A(\hat{\mathbf{r}}, u^{\rm i}) = \frac{1}{4\pi} \sum_{j=1}^{m}\sum_{k=1}^{m} \left[\delta_{j,k}\omega^2\nu_k + (1-\delta_{j,k})\omega^4\nu_j\nu_k\mathcal{G}(\mathbf{r}_j,\mathbf{r}_k)\right] u^{\rm i}(\mathbf{r}_k)e^{-i\omega\hat{\mathbf{r}}\cdot\mathbf{r}_j} \tag{123}$$

where $u^{\rm i}$ is not necessarily a plane wave.

In the case of a plane wave incidence (2) we observe the symmetry between the incident and scattered plane waves in (123). Therefore, reversing and interchanging roles of the incident and scattered waves do not affect the scattering amplitude, i.e. $A(\hat{\mathbf{r}}, \mathbf{d}) = A(-\mathbf{d}, -\hat{\mathbf{r}})$. This is the reciprocity referred to in Section 2.2.

In the case of a point sensor located at $\mathbf{r}_0$ and an incident plane wave, the measurement data is given by

$$u^{\rm s}(\mathbf{r}_0) = \sum_{j=1}^{m}\sum_{k=1}^{m} \left[\delta_{j,k}\omega^2\nu_k + (1-\delta_{j,k})\omega^4\nu_{i_j}\nu_k\mathcal{G}(\mathbf{r}_j,\mathbf{r}_k)\right] e^{i\omega\mathbf{d}\cdot\mathbf{r}_k}G(\mathbf{r}_0,\mathbf{r}_j) \tag{124}$$

whose right hand side can also be interpreted as the scattering amplitude in the direction $-\mathbf{d}$ when a point source is placed at $\mathbf{r}_0$, i.e. $A(-\mathbf{d}, u^{\rm i})$ with $u^{\rm i}(\mathbf{r}) = G(\mathbf{r},\mathbf{r}_0)$. This is the reciprocity referred to in Section 2.5.

E-mail address: fannjiang@math.ucdavis.edu

Department of Mathematics, University of California, Davis, CA 95616-8633